Prell, W. L., Niitsuma, N., et al., 1991
Proceedings of the Ocean Drilling Program, Scientific Results, Vol. 117

23. THE INORGANIC GEOCHEMICAL RECORD OF THE NORTHWEST ARABIAN SEA: A HISTORY OF PRODUCTIVITY VARIATION OVER THE LAST 400 K.Y. FROM SITES 722 AND 724[1]

Graham B. Shimmield[2] and Stephen R. Mowbray[2]

ABSTRACT

High-resolution sampling from late Pleistocene (last 400 k.y.) sediments of Site 722 (upper 16 m) and Site 724 (upper 70 m), and subsequent inorganic geochemical analysis, has defined the history of productivity in the northwest Arabian Sea. Eolian dust input from the Arabian Peninsula and Somalia is characterized by the record of Ti/Al and Cr/Al. This dust record displays strong precessional periodicity (cycles at 25 k.y.) suggesting the Southwest Monsoon and associated winds play a key role in transporting terrigenous material from the land. High biological productivity results in the accumulation of biogenic $CaCO_3$ and opal in the sediments, the latter having an unexpectedly minor contribution to the total mass flux. Due to dilution of the $CaCO_3$ record by the terrigenous component, the record of biological productivity is best exemplified by Ba. Its record, together with that of other metals recording biological association and redox variability (Cu, Ni, Zn, V, U) clearly identifies the interglacial episodes as being more biologically productive. The striking agreement between Ba and the $\delta^{18}O$ record in planktonic foraminifers suggests that the supply of nutrients during these periods of high productivity is linked to ocean-wide changes in ocean fertility, and not just local upwelling conditions. High levels of phosphate accumulation in interglacial sediments is attributed to both diagenetic phosphorite formation and biogenic skeletal debris. This study provides a detailed record of productivity variation in the northwest Arabian Sea during the late Pleistocene.

INTRODUCTION

The northwest Arabian Sea has been long known as an area of active oceanic upwelling, brought about by the seasonal Southwest Monsoon (Sen Gupta et al., 1975; Rao and Jayaraman, 1970; Qasim, 1982; Slater and Kroopnick, 1984). The intensity of this wind induces Ekman transport of surface waters in the summer months and sustains high levels of biological productivity through nutrient supply from intermediate water depths. Microbial decay of the settling organic matter creates an intense oxygen minimum zone (OMZ) between depths of 200 and 1500 m.

As significant variations in the climate of the Earth have occurred during the late Pleistocene (CLIMAP, 1976), and the Southwest Monsoon is believed to have been strongly influenced by glacial/interglacial episodes (Prell, 1984a; Prell and Kutzbach, 1987), it is likely that the sediments underlying the upwelling zone will record the history of the productivity variations driven by the Southwest Monsoon. Previous studies have used "proxy-indicators" such as the distribution of pollen types and the percentage of *G. bulloides* in sediment cores to elucidate the history of upwelling (Van Campo et al., 1982; Prell, 1984a, b; Prell and Van Campo, 1986) with some success. However, inorganic geochemistry as applied to paleoceanography and climate change pioneered in the Pacific (Adelseck and Anderson, 1978; Pedersen, 1983; Lyle et al., 1988; Pedersen et al., 1988; Finney et al., 1988) has not been applied to the northwest Indian Ocean. Surface sediment geochemistry of this area (Kolla et al., 1981; Shankar et al., 1987; Shimmield et al., 1990) has provided a geochemical framework delineating the importance of terrigenous dust inputs together with skeletal $CaCO_3$ and minor opal accumulation in this area.

In this study we have selected two sites from the Oman Margin and performed a high-resolution study of the inorganic geochemistry recorded in the sediments accumulating over the past 400,000 yr. By using simple statistical treatment (principal component analysis) of the data we are able to define four major factors accounting for 80%–95% of the geochemical variation observed. Interpretation of the depth profiles of key elements, together with spectral analysis (see Weedon and Shimmield, this volume) allows an assessment of the significance of the Southwest Monsoon and changes in global climate in influencing the history of upwelling productivity.

SAMPLING AND METHODS

Two sites were selected for this high-resolution study of the inorganic chemical composition of late Pleistocene sediments. These represent depositional conditions on the Owen Ridge below the present position of the OMZ (Site 722) in 2028 m of water, and within the OMZ on the Oman continental margin (Site 724) in 593 m of water (Fig. 1). At both sites only the upper (I) lithologic unit was sampled which was composed of foraminifer-bearing nannofossil ooze (5%–25% foraminifers) at Site 722, and calcareous clayey silt with 5%+ foraminifers at Site 724. Over the depth intervals studied here (0–15 mbsf, Hole 722B; 0–68 mbsf, Hole 724C), the sedimentary sequence is essentially homogeneous with respect to mineralogical composition and sedimentary structures. No evidence of slumped horizons, or mass flow deposits are noted (Shipboard Scientific Party, 1989a, b) and the units sampled were undisturbed by gas expansion voids.

On vertical sectioning of the cores, 20 cm^3 plugs were taken at 20 cm intervals from both holes, and sealed in polyethylene bags. On arrival at Edinburgh the samples were stored at 4°C prior to processing. Water contents were measured by weight loss on drying at 60°C. Using an average grain density of 2.6 g cm^{-3} (Shipboard Scientific Party, 1989a, b), dry bulk density values were calculated for use in flux calculations. In addition, sea salt concentrations were estimated assuming a pore water salinity equivalent to normal seawater. All chemical data presented here are corrected for sea salt dilution (and contribution in the case of Mg and Ca).

The bulk sediment samples were ground in a tungsten carbide Tema mill and prepared for X-ray fluorescence spectrome-

[1] Prell, W. L., Niitsuma, N., et al., 1991. *Proc. ODP, Sci. Results*, 117: College Station, TX (Ocean Drilling Program).

[2] The Department of Geology and Geophysics, University of Edinburgh, West Mains Road, Edinburgh, EH9 3JW, Scotland, U.K.

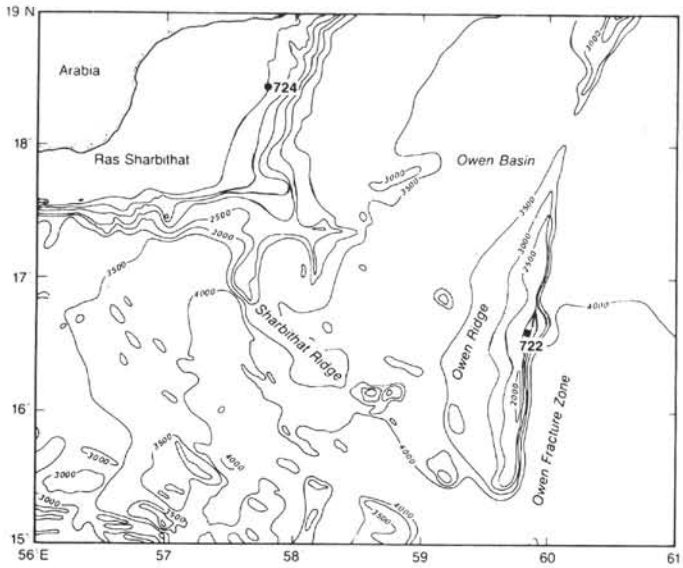

Figure 1. Location of Sites 722 and 724 in the northwest Arabian Sea.

try (XRF). This involved the fusion of the sediment powder into a glass disc using lithium tetraborate and La as a heavy absorber (Norrish and Hutton, 1969) for major elements, and pressing the powder into a briquette with boric acid backing for minor elements (Shimmield, 1985). The XRF analysis was performed on a Phillips PW1250 sequential automatic X-ray spectrometer. International rock standards were used for calibration. The precision and accuracy of the method are given in Table 1. For U and Th data, α-spectrometry was performed on total dissolution of the sample using isotope dilution. The extremely precise methodology is reflected in the presentation of data to two significant figures (for further details see Shimmield and Mowbray, this volume).

RESULTS AND DISCUSSION

The bulk chemical data obtained from the late Pleistocene sediments in Holes 722B and 724C are given in Appendixes A–C. Major element data are presented for both holes. At Site 722 we also present minor element data, providing a detailed geochemical record over the last 365 k.y. Appendix D presents minimum, average, and maximum major element values and trace element values for Holes 722B and minimum, average, and maximum major element value for Hole 724C. Late Pleistocene/Holocene stratigraphy is provided by the $\delta^{18}O$ record of planktonic foraminifers, courtesy of Prell et al. (this volume) and Pedersen and Zahn (this volume) for Holes 722B and 724C, respectively (Fig. 2). Age assignments are based on the correlation of the $\delta^{18}O$ curve with the SPECMAP stack (Imbrie et al., 1984). The age models from these authors were also used to generate linear sedimentation rates from which we calculate mass accumulation rates based on our dry bulk density values.

In the Arabian Sea, the bulk sediment composition is controlled by both lithogenic and biogenic input, with virtually no hydrothermal component (Shankar et al., 1987; Shimmield, et al., 1990). Consequently, these data are presented as element-to-aluminum ratios in order to examine fluctuations in the chemistry of the aluminosilicate component that are not due to variations in the biogenic component.

In order to examine the first-order relationships and controls on the geochemical composition of the Pleistocene sediments, statistical analysis of the complete dataset on both holes has been performed. Table 2 presents the results of inter-element correlation, while Table 3 indicates the results of principal component analysis (a data reduction technique for identifying a small set of variables that account for a large proportion of the total variance in the original variables). In Table 3 it is apparent that the first three eigenvalues (i.e., the variance of the principal components) account for 94.6% of the total variance in major element composition for Hole 724B, and 80.4% of the total

Table 1. XRF and α-spectrometry analytical precision and accuracy for major and minor elements.

Element	Mean (n = 8)	1σ	Estimated total precision[a] (as % rel. std. dev., 1σ)	Accuracy[b]
Si	26.24	0.12	0.5	0.097
Al	7.99	0.03	0.4	0.075
Fe	5.29	0.03	0.6	0.032
Ca	1.14	0.01	1.0	0.048
K	2.39	0.01	0.4	0.019
Ti	0.45	0.004	1.0	0.009
Mn	2.15	0.02	0.7	0.004
P	0.10	0.002	2.0	0.013
Ba	2736	36.83	1.3	42.5
Ce	73	1.20	1.6	13.5
Cr	107	1.83	1.7	14.4
Cu	112	0.83	0.7	4.7
Nd	34	0.90	2.6	3.6
Ni	120	0.71	0.6	4.7
Rb	80	0.43	0.5	3.8
Sr	400	3.77	0.9	10.7
V	114	2.11	1.8	10.8
Y	30	0.43	1.4	3.8
Zn	193	0.99	0.5	6.1
Zr	126	1.12	0.9	7.2

α-Spectrometry Analytical Precision and Accuracy

Element	Mean[c] (n = 6)	1σ	% r.s.d.	Accuracy
U	2.73	0.17	6.2	0.05
Th	9.22	0.33	3.6	0.05

Major element mean concentrations and accuracy in wt.%, minor elements in ppm.

[a] Total precision includes counting error, disc reproducibility, error in regression line, and error in matrix mass absorption determinations.

[b] Accuracy determined from r.m.s.d. of international standards about the regression line.

[c] Mean concentration and accuracy expressed in ppm.

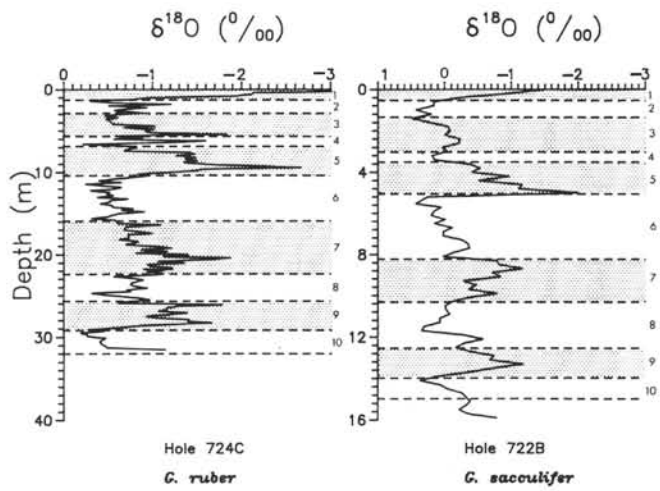

Figure 2. Oxygen isotope stratigraphy for Hole 724C (Zahn and Pedersen, this volume) and Hole 722B (Clemens and Prell, this volume). Isotope stages assigned by matching to the SPECMAP stack (Imbrie et al., 1984). In this, and following figures, odd numbered interglacial stages are shaded.

Table 2. Correlation matrix, Holes 722B and 724C.

	Hole 722B																			
	Si	Al	Fe	Ti	Mn	P	Ca	Ni	Cr	V	Cu	Zn	Sr	Rb	Zr	Ba	Ce	Nd	Y	U
Al	0.979																			
Fe	0.964	0.979																		
Ti	−0.969	−0.955	−0.954																	
Mn	0.982	0.993	0.976	−0.958																
P	0.839	0.852	0.834	−0.792	0.849															
Ca	0.540	0.538	0.567	−0.515	0.560	0.450														
Ni	0.836	0.830	0.856	−0.812	0.834	0.668	0.514													
Cr	0.910	0.904	0.911	−0.880	0.917	0.721	0.557	0.863												
V	0.828	0.843	0.836	−0.777	0.823	0.691	0.408	0.827	0.857											
Cu	−0.081	−0.056	−0.051	0.169	−0.071	−0.170	0.031	0.197	0.121	0.241										
Zn	0.623	0.617	0.609	−0.573	0.604	0.457	0.337	0.737	0.680	0.735	0.446									
Sr	−0.787	−0.768	−0.771	0.821	−0.786	−0.700	−0.425	−0.527	−0.640	−0.495	0.267	−0.348								
Rb	0.918	0.940	0.927	−0.879	0.924	0.754	0.505	0.850	0.939	0.919	0.126	0.707	−0.602							
Zr	0.788	0.797	0.786	−0.731	0.803	0.627	0.480	0.740	0.881	0.805	0.126	0.585	−0.379	0.882						
Ba	−0.499	−0.545	−0.520	0.521	−0.556	−0.533	−0.343	−0.234	−0.432	−0.256	0.426	0.052	0.429	−0.466	−0.496					
Ce	0.568	0.573	0.583	−0.562	0.560	0.415	0.316	0.574	0.607	0.592	0.079	0.393	−0.372	0.628	0.539	−0.238				
Nd	0.241	0.234	0.232	−0.203	0.222	0.074	0.143	0.347	0.305	0.335	0.269	0.337	−0.018	0.347	0.297	0.047	0.509			
Y	0.529	0.560	0.561	−0.457	0.539	0.297	0.317	0.681	0.662	0.774	0.522	0.718	−0.143	0.712	0.672	0.026	0.472	0.469		
U	0.015	0.010	0.020	−0.029	0.018	−0.036	−0.004	0.083	0.066	0.089	0.240	0.083	−0.005	0.030	0.072	0.218	0.071	−0.002	0.191	
Th	0.645	0.647	0.692	−0.646	0.651	0.592	0.392	0.676	0.667	0.636	0.025	0.396	−0.361	0.648	0.621	−0.409	0.471	0.177	0.354	−0.059

	Hole 724C							
	Si	Al	Fe	Mg	Ca	K	Ti	Mn
Al	0.908							
Fe	0.782	0.960						
Mg	0.785	0.882	0.888					
Ca	−0.871	−0.899	−0.853	−0.825				
K	0.901	0.984	0.954	0.926	−0.904			
Ti	0.933	0.971	0.923	0.882	−0.906	0.969		
Mn	0.832	0.866	0.837	0.858	−0.790	0.879	0.878	
P	−0.382	−0.451	−0.476	−0.520	0.374	−0.491	−0.465	−0.521

Table 3. Eigenanalysis of correlation matrix of Holes 722B and 724C.

			Hole 722B			
Eigenvalue	12.354	3.640	1.099	0.835	0.766	0.533
Proportion	0.588	0.173	0.052	0.040	0.036	0.025
Cumulative	0.588	0.762	0.814	0.854	0.890	0.916
Variable	PC1	PC2	PC3	PC4	PC5	PC6
Si	0.273	0.111	0.046	0.002	−0.057	−0.139
Al	0.274	0.105	0.051	−0.005	−0.084	−0.141
Fe	0.275	0.087	0.037	0.002	0.021	−0.019
Ti	−0.266	−0.138	−0.057	−0.034	0.076	0.110
Mn	0.272	0.127	0.054	0.009	−0.032	−0.139
P	0.216	0.209	0.149	−0.140	−0.071	0.068
Ca	0.153	0.106	−0.146	0.054	0.892	−0.012
Ni	0.259	−0.154	0.007	−0.130	0.113	0.092
Cr	0.275	−0.052	−0.035	0.055	0.019	−0.022
V	0.259	−0.138	0.068	−0.035	−0.200	0.076
Cu	0.031	−0.437	0.178	−0.231	0.160	0.004
Zn	0.172	−0.274	0.090	−0.474	0.020	−0.200
Sr	−0.121	−0.419	−0.260	−0.031	0.081	0.040
Rb	0.276	−0.081	−0.046	0.000	−0.084	−0.073
Zr	0.270	−0.119	−0.076	0.032	0.008	−0.091
Ba	−0.150	−0.342	0.214	−0.094	−0.108	0.132
Ce	0.207	−0.108	−0.131	0.448	−0.195	0.290
Nd	0.115	−0.304	−0.398	0.439	−0.004	0.004
Y	0.189	−0.351	−0.013	0.021	−0.030	−0.166
U	−0.006	−0.158	0.775	0.477	0.190	0.011
Th	0.203	0.051	0.032	−0.212	0.055	0.851
			Hole 724C			
Eigenvalue	7.658	1.068	0.566	0.235	0.201	0.134
Proportion	0.766	0.107	0.057	0.023	0.020	0.013
Cumulative	0.766	0.873	0.929	0.953	0.973	0.986
Variable	PC1	PC2	PC3	PC4	PC5	PC6
Si	−0.334	−0.169	−0.002	−0.634	0.027	0.102
Al	−0.354	−0.025	0.122	0.047	−0.151	0.355
Fe	−0.341	0.086	0.179	0.456	−0.185	0.362
Mg	−0.336	0.083	−0.003	0.495	0.267	−0.495
Ca	0.333	0.089	−0.175	0.202	0.452	0.661
Na	−0.162	−0.733	−0.618	0.177	0.034	0.025
K	−0.357	0.017	0.092	0.107	−0.085	0.109
Ti	−0.354	−0.026	0.087	−0.138	−0.082	0.194
Mn	−0.329	0.125	0.037	−0.180	0.784	−0.030
P	0.189	−0.628	0.723	0.092	0.191	−0.005

variance for major, minor, and trace element data in Hole 722B. In Figures 3 and 4 the principal component scores of the compositional data are plotted on the first two, and on the first and third, principal components (cf., Li, 1982). According to Figures 3 and 4, the geochemical data broadly define four major phase associations; (1) aluminosilicate detritus (Al, K, Fe, Rb, Th, Ti, Cr, Zr, V), (2) biogenic carbonate (Ca, Sr), (3) organic matter (Ba, Cu, U), and (4) phosphatic material (P, Y, Ce, Nd). The remaining elements (Si, Mn, Cu, Ni, Zn) show relationships with both biogenic and lithogenic sources. We will now describe the distribution of the elements in detail, and account for their association.

Aluminosilicate Detritus Factor

The characteristic element defining this phase group is Al which is principally derived from aluminosilicate clay minerals. These clay minerals may be of terrestrial origin, or from alteration of oceanic basalts and/or hydrothermal exhalations (McMurtry and Yeh, 1981; Bonatti et al., 1983; Shankar et al., 1987; Nath et al., 1989). From studies on the distribution of sediment type on the Oman continental margin (Shimmield et al., 1989; Sirocko and Sarnthein, 1989) we consider that Al may be used as an exclusive indicator of clay detritus of continental terrigenous origin.

Preliminary results (Shipboard Scientific Party, 1989a, b) and Debrebant (this volume) indicate that illite and chlorite (and kaolinite?) with minor amounts of palygorskite form the dominant clay mineralogy. Kolla et al. (1981) have shown that palygorskite and illite are rather ubiquitous in the northwest Arabian Sea being deposited via eolian transport, the former originating in soils of the Arabian Peninsula and Somalia. From the preliminary principal component analysis we note the close association of Fe, K, Rb, Th, Zr, V, Ti, and Cr with Al. This composition of the aluminosilicate detritus, but also suggest how this composition may have varied with time (see discussion below). The Fe, K, Rb, and Th content of the terrigenous component is rather constant over the depth sampled (Figs. 5 and 6) being strongly controlled by the illite/chlorite mineralogy (Boyle, 1983; Shankar et al., 1987). This agrees well with the rather uniform K and Th results and interpretation obtained by the downhole logging of Unit I (Shipboard Scientific Party, 1989a, b). The Zr/Al profile indicates strong spikes corresponding to similar excursions in the Ti/Al and Cr/Al profiles. We interpret these as concentrations of heavy minerals (see below). V/Al displays a depth profile in Hole 722B that suggests elevated V content within interglacial stages (particularly 1, 5, and 7). While, there is a first-order association with aluminosilicate detritus, V may well be concentrated in the sediment during periods of high organic matter flux via redox processes (Bonatti et al., 1971;

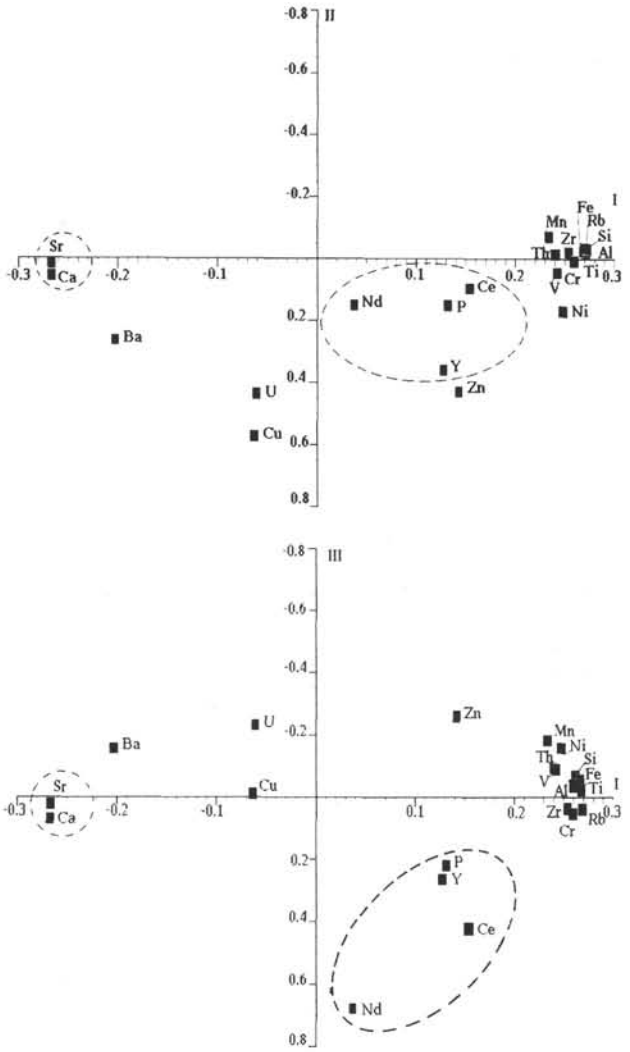

Figure 3. Plots of the principal component factors 1 vs. 2 and factors 1 vs. 3 for Hole 722B.

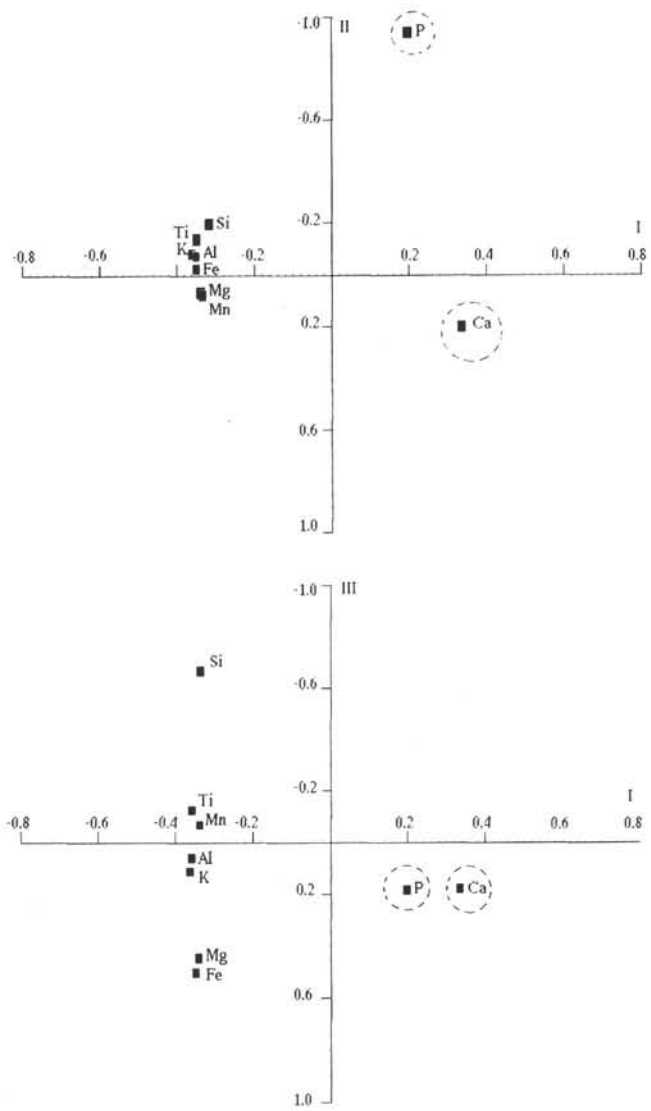

Figure 4. Plots of the principal component factors 1 vs. 2 and factors 1 vs. 3 for Hole 724C.

Thomson et al., 1987). We address this point further below. However, the detailed variation in Ti/Al and Cr/Al bears close examination. It is clear from Figure 5 that both elements in the aluminosilicate detritus covary to a high degree (Cr:Ti correlation of 0.931) and that a high frequency oscillation is present. This downcore variation is not related to glacial/interglacial cycles in a simple way (glacial stages are shaded in Fig. 5). By the use of fast Fourier transform (FFT) spectral analysis (see Weedon and Shimmield, this volume, for details) we have resolved the major oscillation component into a 25 k.y. cycle for both Ti/Al and Cr/Al in Hole 722B (using the age model of Prell et al., this volume) shown in Figure 7. Ti/Al also responds to minor 100 k.y. and 41 k.y. forcing. However, the dominant periodicity at the precession band suggests that an important influence on Ti/Al and Cr/Al variation is the Southwest Monsoon by analogy with other proxy-indicators that have been shown to display similar forcing (Prell and Kutzbach, 1987).

To evaluate more fully the signal contained in the Ti and Cr ratios, we must assess their geochemical pathway. Ti is known to be preferentially concentrated in coarser sediment fractions (Spears and Kanaris-Sotiriou, 1976; Schmitz, 1987) due to its incorporation into heavy minerals such as ilmenite, rutile, titanomagnetite, and augite. Cr is an important minor element constituent of the ultrabasic rocks making up the serpentinites of the Oman ophiolite on the Arabian Peninsula and nearby Masirah Island (Moseley and Abbotts, 1979). It is proposed that the variation in ratio observed downcore may result from changes in wind intensity (and possible small changes in direction) affecting the aerodynamics of the heavy mineral transport. This situation is most likely at Site 722 on the crest of the Owen Ridge where downslope sediment transport and variations in fluvial runoff are much less likely. Boyle (1983) pioneered the use of Ti/Al as an indicator of climate change from his work on sediment accumulation under the Peru Current. He proposed that Ti/Al fluctuations could be attributed to changes in the intensity of eolian transport associated with glacial/interglacial cycles. From our results presented here, and the studies of these earlier workers, we interpret the oscillation in Ti/Al (and Cr/Al) as a direct indicator of monsoon strength over the late Pleistocene, and that the dominant 25 k.y. precession cycle plays an important role.

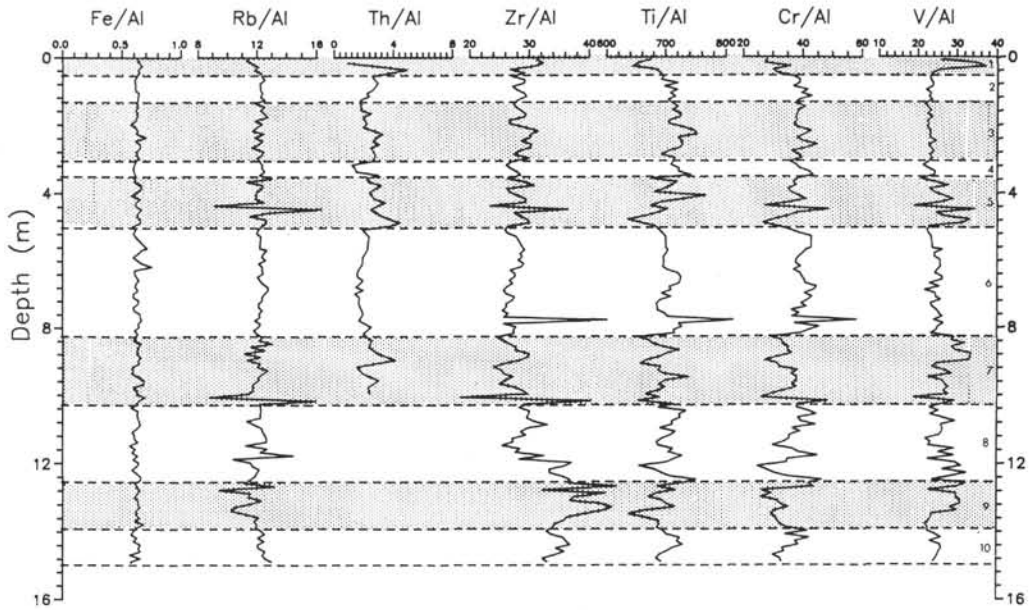

Figure 5. Element-to-Al weight ratios comprising the aluminosilicate detritus factor with depth in Hole 722B. All ratios except Fe/Al are $\times 10^{-4}$.

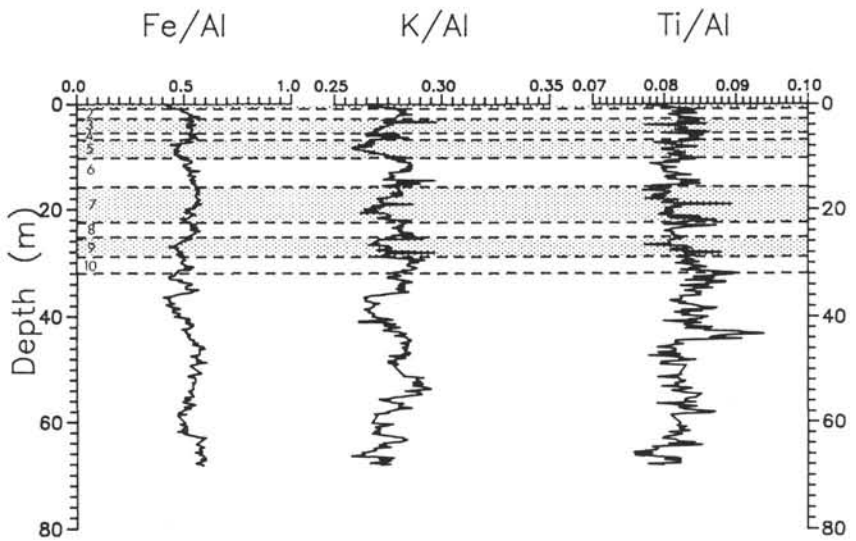

Figure 6. Element-to-Al weight ratios comprising the aluminosilicate detritus factor with depth in Hole 724C.

The Biogenic Component

The calcareous biogenic component at Sites 722 and 724 can be identified by both the total Ca and Sr XRF analysis. We have calculated the $CaCO_3$ content of the sediment samples by subtracting an aluminosilicate Ca component (in proportion to the amount of Al present) and converting the excess Ca to $CaCO_3$. Thus,

$$CaCO_3 = 2.5(Ca_{tot} - (Ca/Al_{clay} \times Al_{tot}))$$

where Ca/Al_{clay} is taken as 0.345 (Turekian and Wedepohl, 1961). This method is in error at very low $CaCO_3$ contents due to uncertainties in the aluminosilicate ratio, but is unrivalled in precision at the 50%–80% $CaCO_3$ level found at these two sites. However, the method cannot distinguish between $CaCO_3$ of *in-situ* marine biogenic origin and detrital $CaCO_3$ from the Arabian Peninsula.

Examination of the downcore record of $CaCO_3$ in Holes 722B and 724C (Fig. 8) reveals that the highest mean $CaCO_3$ content is found at the ridge site, and that interglacial periods generally have higher concentration levels. It is tempting to conclude that carbonate productivity variations are responsible and that interglacial periods were therefore more productive, but consideration of sediment mass accumulation rate (MAR) is important here. Figure 8 displays the MAR for both holes together with

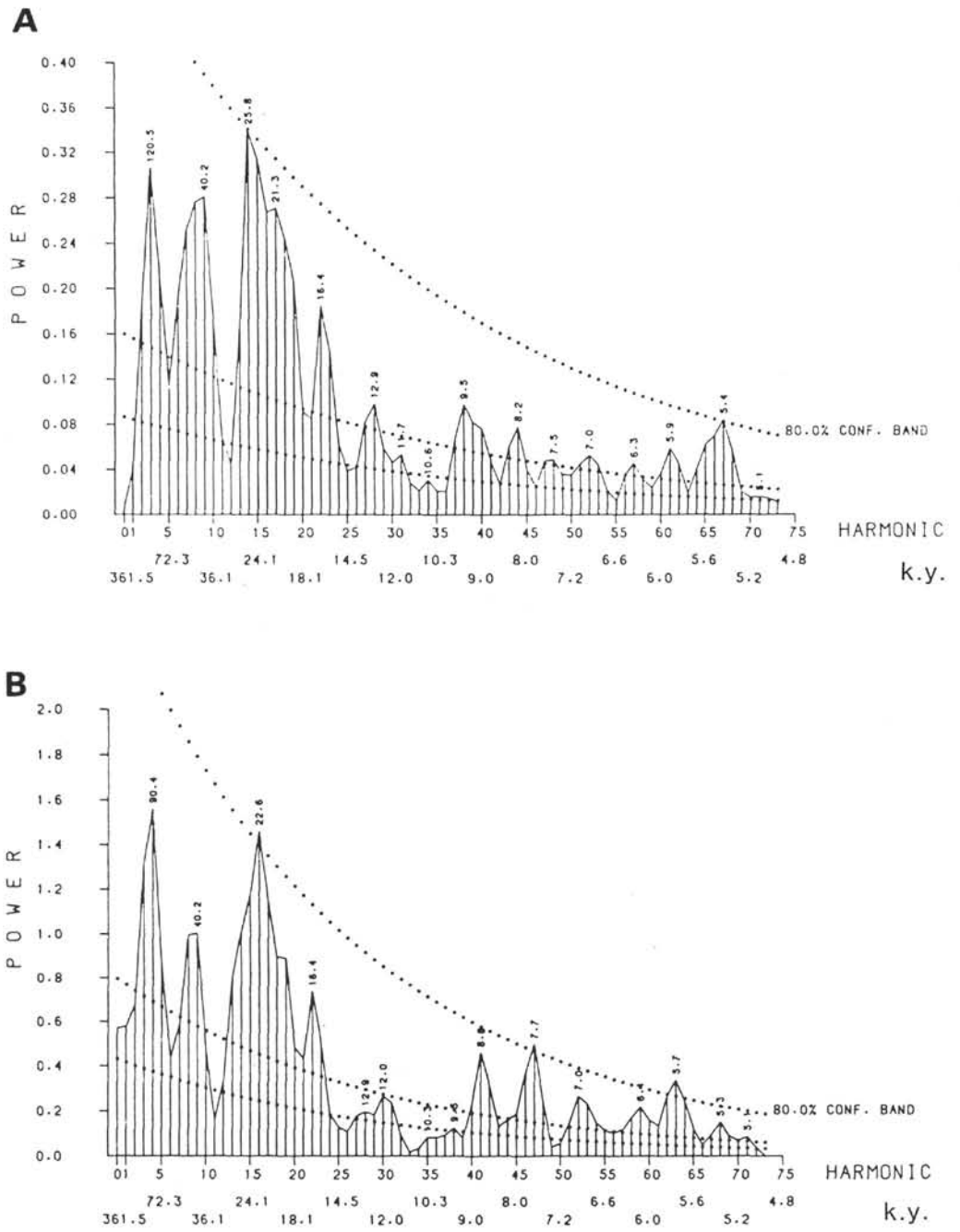

Figure 7. Periodograms for Hole 722B. **A.** Ti/Al. **B.** Cr/Al.

the $CaCO_3$ and terrigenous (1 − $CaCO_3$) content, indicating that the terrigenous component dominates the overall MAR and therefore dilutes the $CaCO_3$ signal antithetically. Higher MAR's occur during glacial possibly as a result of changes in sea level and/or aridity and runoff. In order to identify changes in ocean productivity, through mechanisms such as upwelling, we require a geochemical indicator which would preserve this signal despite dilution by terrigenous material and variation in $CaCO_3$ dissolution on the seafloor, and preferably with a large dynamic range (see below).

Sr is very closely correlated with Ca (Sr:Ca = 0.947, Table 1) in Hole 722B. This is unsurprising as seawater Sr is known to be incorporated into the tests of marine organisms during growth (Table 3). However, the Sr/Ca ratio on the Owen Ridge (Fig. 9) is somewhat higher that has previously been reported and displays an interesting history. Figure 9 displays the close, but damped or modulated, trend of Sr/Ca in comparison with the $\delta^{18}O$ curve. Elevated Sr contents reflect a more negative (heavier) $\delta^{18}O$ signal in the planktonic foraminifer (*Globigerinoides sacculifer*) corresponding to interglacial stages. Perhaps the Sr content of the biogenic $CaCO_3$ is reflecting a temperature or species or vital effect control. We do not believe diagenetic overprinting (Baker et al., 1982) is responsible due to the shallow depth of this core. In addition, marine barite is known to contain Sr (0.2–3.4 mol%; Church, 1979), but the Ba record in Hole 722B (Fig. 11) is unable to account for the Sr/Ca shown in Figure 9.

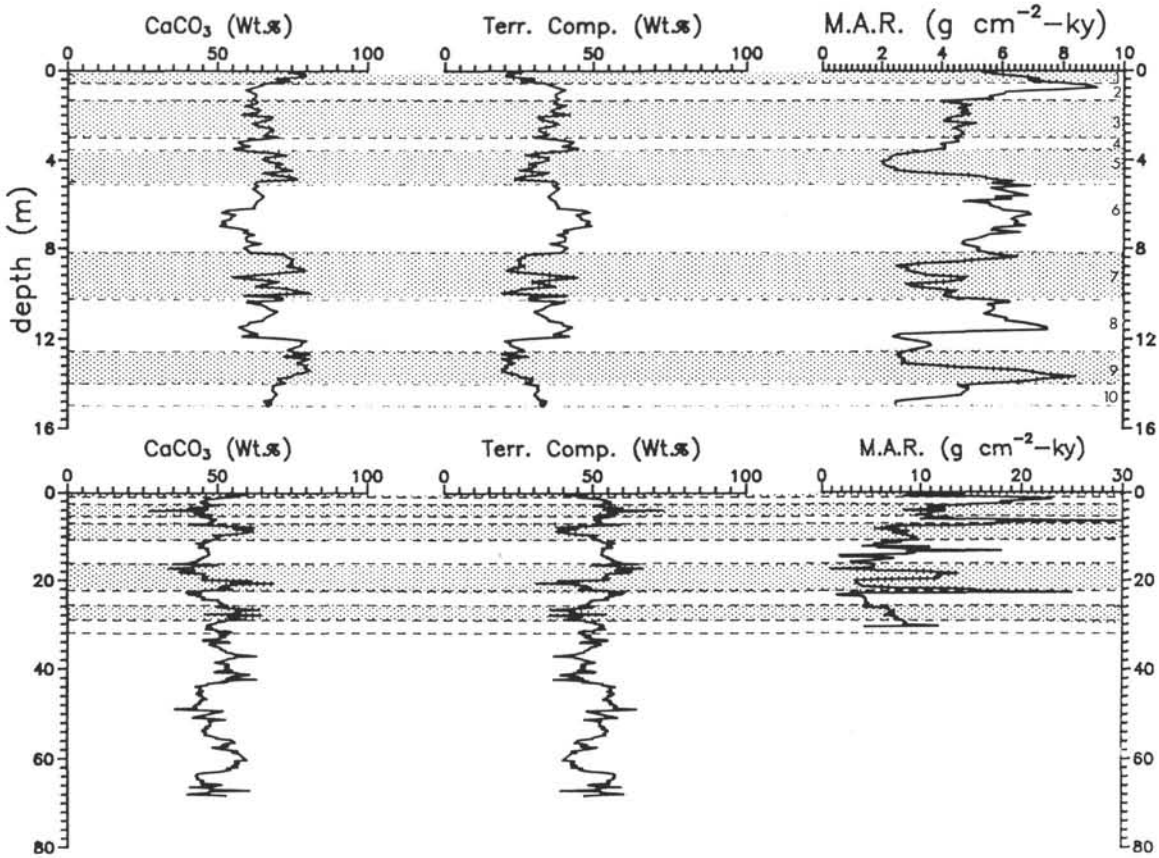

Figure 8. $CaCO_3$ (wt%), terrigenous component (100 − $CaCO_3$; wt%), and mass accumulation rate (g cm^{-2} k.y.$^{-1}$) with depth for Holes 722B (top) and 724C (bottom).

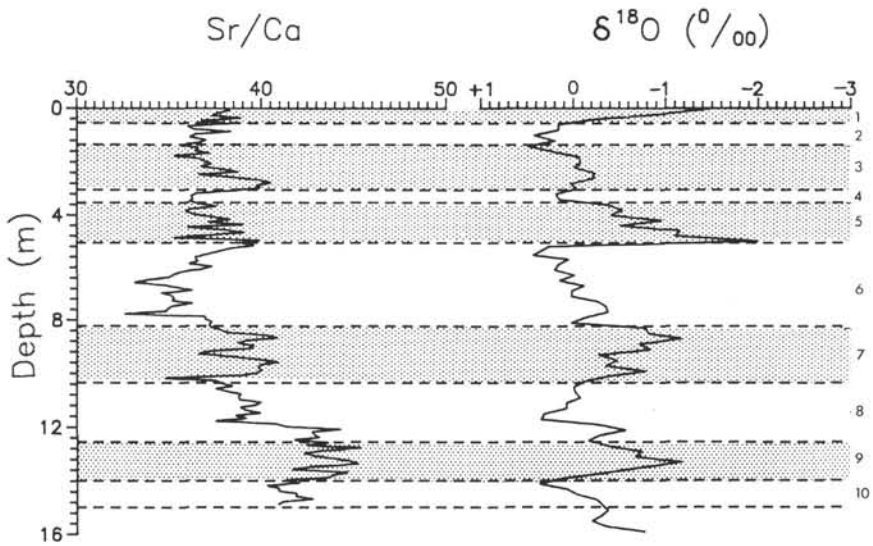

Figure 9. Sr/Ca ($\times 10^{-4}$) weight ratio and $\delta^{18}O$ with depth in Hole 722B.

The content and distribution of Si in these late Pleistocene sediments may be attributed to both detrital terrigenous clays and quartz, and to biogenic opal. Figure 10 displays the depth profiles at Sites 722 and 724. It is immediately apparent that there are two important differences between the sites. At Site 722 the depth profile appears to have a constant Si/Al ratio of 3.8 with occasional major increases (shale has a ratio of 3.4; Turekian and Wedepohl, 1961). At Site 724, however, the overall Si/Al is rather higher (about 5.0) but is variable without such a well defined baseline. However, both sites display high Si/Al ratios in the Holocene section (Stage 1). Labracherie et al. (1983) studied the stratigraphic distribution of diatoms over the last 25 k.y. and has shown that opal productivity was (and is) higher in the Holocene. At Site 722, comparison of the Si/Al record with

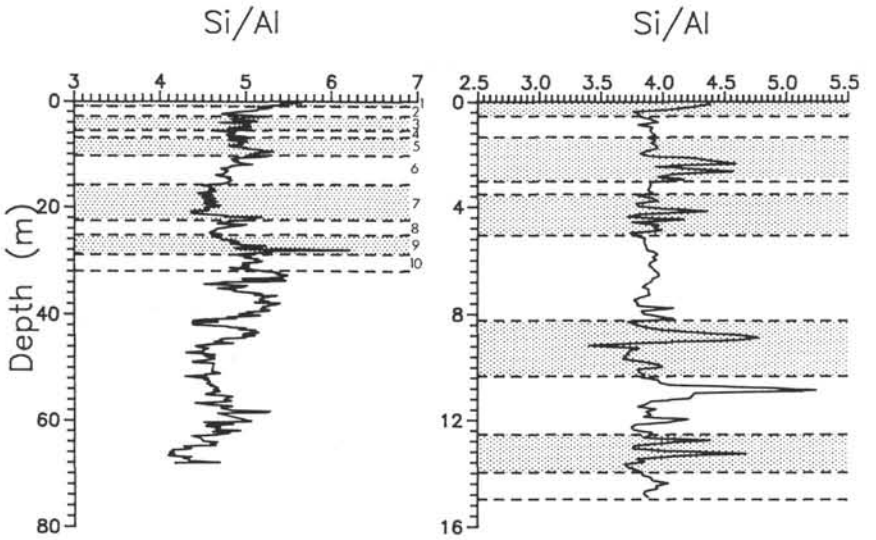

Figure 10. Si/Al (weight ratio) with depth in Holes 722B (left) and 724C (right).

unpublished opal data (determined by wet chemistry) from the site survey core (RC27-61; D. Murray, pers. comm., 1989) suggests that the spikes are indeed due to higher contents of biogenic opal. If this record reflects a constant clay and quartz input, with additions of biogenic opal, then the periodicity of the record (see Weedon and Shimmield, this volume) at 56 k.y. and 25/19 k.y. reflects both precession and an unknown forcing component. The 56 k.y. periodicity has also been observed in SiO_2 records from this leg (S. Clemens, pers. comm., 1989) but remains unexplained. At Site 724 the much higher Si/Al ratio, and the core location on the continental slope, suggests that quartz may be rather more dominant. This is confirmed by smear slide analysis (Shipboard Scientific Party, 1989a, b) which indicates about 10% quartz in Unit I of Hole 724C, and only trace amounts in Hole 722B. Interestingly, the Si/Al profile in Site 724 is antithetically correlated with volume magnetic susceptibility (Shipboard Scientific Party, 1989a, b) suggesting that quartz dilutes the susceptibility record.

Organic Matter (Productivity) Factor

As we have seen above, both $CaCO_3$ and Si are unreliable indicators of the paleoceanographic record of productivity variation in the Arabian Sea. However, one element, Ba, is concentrated by marine organisms and may resist remineralization ("dissolution residue," Dymond, 1981) providing a tracer of paleoproductivity. Since the work of Revelle et al. (1955) many authors have commented on the association of Ba, opal, and biogenic sedimentation. Despite the association of Ba-enriched sediments and regions of upwelling or enhanced productivity, no causal relationship has been definitely established (see review in Schmitz, 1987). Recent studies have suggested that Ba may be in heavy mineral granules functioning as statoliths (Fenchel and Finlay, 1984) within protozoans such as Xenophyophoria and Loxodes (Finlay et al., 1983). Very recently, Ba has been the subject of study in marine particles from the Gulf Stream (Bishop, 1988) and within the calcareous tests of benthic foraminifers (Lea and Boyle, 1989) and corals (Lea et al., 1989). Within the Indian Ocean the recent study of Schmitz (1987) has illustrated the use of Ba as a tracer of plate movement beneath the equatorial upwelling zone on a time scale of millions of years. To our knowledge there is no high-resolution record of Ba from an upwelling area influenced by climate change over a time scale of thousands of years.

Figure 11 illustrates the variation with depth of Ba/Al at Site 722B on the Owen Ridge. The record is striking for two reasons: (1) the Ba/Al has the largest dynamic range of any chemical variable measured here, and (2) the profile bears an almost perfect correlation with the $\delta^{18}O$ stratigraphy. Clearly, elevated Ba contents are found during interglacial stages and must therefore reflect periods of enhanced productivity. (This conclusion holds even when considered in terms of flux, given the higher MAR of glacial periods. This is the advantage of having a tracer with so large a dynamic range.) In Figure 12 a periodogram of Ba/Al displays the strong 100 k.y. cycle that is apparent in the depth profile. As well as eccentricity cycle, both tilt (42 k.y.) and precession (23/16 k.y.) are in evidence, again confirming the similarity of the Ba profile to the $\delta^{18}O$ record. The phasing of this record is discussed further in Weedon and Shimmield (this volume).

From wind strength indicators (e.g., Ti/Al) we believe that the monsoon responds to forcing in the precession band. As upwelling is linked through Ekman transport to wind stress, it is expected that Ba, as a productivity indicator, should also display similar precessional forcing. The fact that longer cycle ("global") forcing is also very evident suggests that nutrient supply to the northwest Arabian Sea may be important. In this context, recent models on deep and intermediate water ventilation or stagnation are pertinent (Keir, 1988; Duplessy et al., 1988) as shown by Cd/Ca tracers in benthic foraminifers (Boyle, 1986). Recent work by Boyle (1988) and Boyle and Keigwin (1987) has shown that intermediate waters in the North Atlantic became nutrient depleted together with reduced North Atlantic Deep Water Flux during the last glacial episode. As the predominant source of nutrients in this area is through upwelling of intermediate waters, changes in the nutrient profile of open ocean waters during glacial time may account for the weaker glacial productivity identified from the Ba/Al signal. Further paleoceanographic studies should concentrate on establishing the nutrient levels of Indian ocean intermediate waters.

In addition to Ba as a direct indicator of changing productivity, the associated organic matter detritus will also affect the sediment geochemistry, either through direct metal complexing or through redox chemistry. Recently, studies by Thomson et al. (1987) have shown the importance of progressive redox fronts in preserving minor metal profiles in non-steady state conditions. Finney et al. (1988) have argued for productivity-induced redox

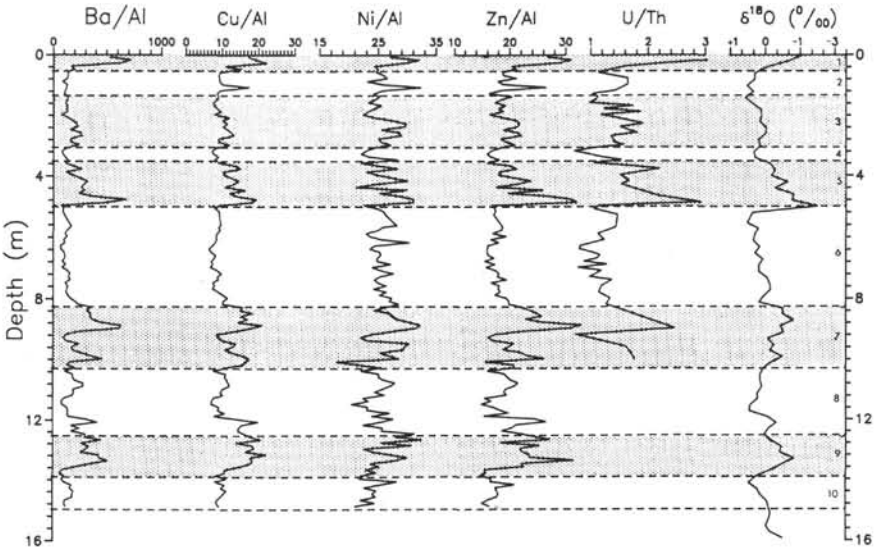

Figure 11. Element-to-Al weight ratios comprising the productivity factor with depth in Hole 722B, together with the $\delta^{18}O$ stratigraphy. All ratios are $\times 10^{-4}$ except U/Th.

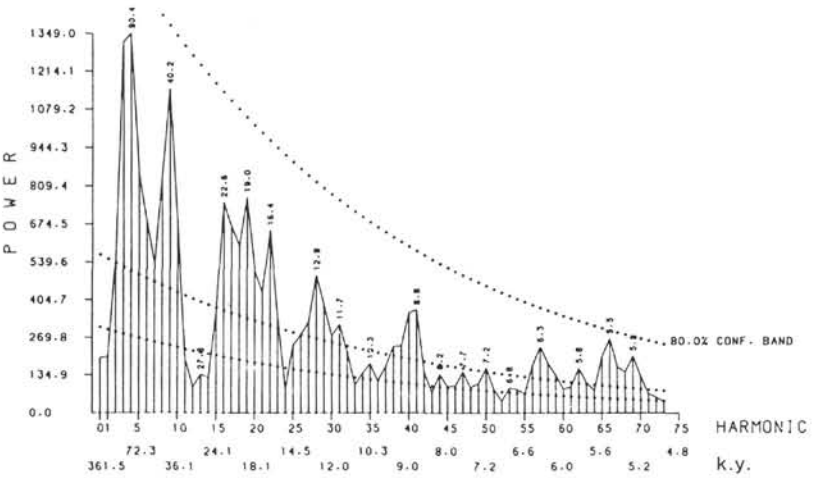

Figure 12. Ba/Al periodogram for Hole 722B.

variations in controlling transition metal distributions in sediments from the eastern equatorial Pacific. In Figure 11, U and Cu are both enriched relative to aluminosilicate levels at depths corresponding to higher productivity periods (defined by Ba/Al). As these two metals (and V) are often associated with more reducing conditions brought about by higher organic matter fluxes (or expansion of the OMZ to intersect the ridge crest) this observation is consistent. The weaker association of Ni/Al and Zn/Al is possibly incurred as particulate organic matter is known to be an effective scavenger of transition metals. The importance of subsurface redox fronts and accumulation rate fluxes is discussed further in Shimmield and Mowbray (this volume). Sediment trap studies in the Sargasso Sea (Jickells et al., 1984) have demonstrated the very close association of Cu, Ni, V, and Zn (also Fe, Mn, P, and Pb) fluxes with total organic carbon flux. They attribute the close association to seasonality driven by changes in primary productivity in the overlying surface waters. Particulate forms of the elements are rapidly consolidated and sedimented with the organic matter.

Phosphatic Factor

The occurrence of phosphatic material accumulating in sediments underlying upwelling zones has been long recognized (Burnett, 1977; and others). This material may be diagenetic in origin, or of biogenic skeletal (fish teeth and bones) nature. Both phases are known to concentrate the rare earth elements. In Figure 3 the clear association of P with Ce, Y, and Nd may be seen. Similar statistical analysis by Li (1982) also recognized the existence of phosphate minerals and REE's in sediments. At Site 722 the phosphatic sediments (identified by the P/Al ratio) are more common during interglacial stages (Fig. 13) with an average P/Al ratio of 0.025 in the upper 16 m. We may attribute this distribution to the effect of elevated interglacial productivity, as identified by the tracers described above. However, at Site 724 a rather different distribution is recorded (Fig. 13). Here the baseline P/Al ratio is roughly the same (0.02–0.03) but highly enriched phosphate horizons (reaching a maximum P/Al of ~0.4) are recorded. These enriched horizons also occur within

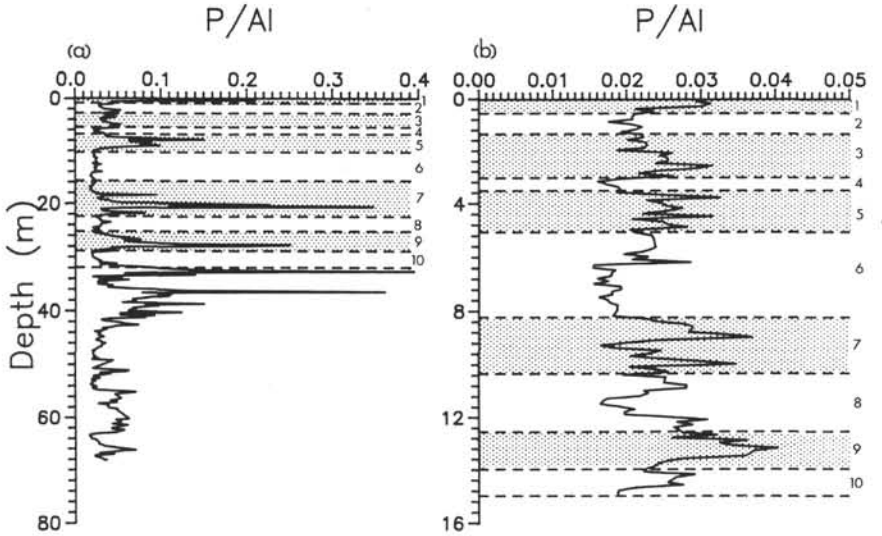

Figure 13. P/Al weight ratio with depth for Holes 722B (left) and 724C (right).

interglacial sediments suggesting their origin is also linked to high productivity episodes. The phase containing the phosphate is unknown, but phosphate nodules at a depth of about 44 m were recorded by the Shipboard Scientific Party (1989b) in Hole 724A.

CONCLUSION

The results presented here together with their interpretation suggest that the Oman margin has experienced major changes in productivity and upwelling history during the late Pleistocene. Through the use of high-resolution inorganic geochemistry, together with a unique sedimentary record provided by hydraulic piston coring, we have been able to define the pattern of these climate changes.

The Southwest Monsoon (and associated northwest winds—the Shamal; Sirocko and Sarnthein, 1989) appears to be responsible for the bulk of the eolian dust input to the northwest Arabian Sea. This dust input may be clearly identified by the Ti/Al and Cr/Al record, and occurs with a frequency that suggests forcing by orbital precession. This result is in agreement with other proxy-indicators that have been shown to display similar forcing (Prell and Kutzbach, 1987).

The record of biogenic productivity is more involved, responding to both local upwelling intensity and changes in the global ocean/climate system. The record of bulk biogenic carbonate is strongly influenced by, and inversely correlated with, terrigenous aluminosilicate detritus. Some biogenic silica occurs at Site 722. Using time series analysis, the opal distribution curves reflect both precession and an unknown forcing component at 56 k.y. The dominant contribution to the total Si measured in these sediments is from clay and quartz. The question of why an upwelling area that at the present day supports high opal productivity (diatoms), but fails to record changes in this opal productivity within the sediments, requires further study.

In this study Ba has proved to be an excellent indicator of changes in productivity with time. The record closely follows the $\delta^{18}O$ signal recorded in planktonic foraminifers, suggesting that not only local upwelling, but ocean-wide changes in nutrient supply, may influence the biological community. Responding to these changes in productivity is the flux of biological detritus (fecal material, tissue, skeletons) to the sediments, which drive redox variations in the sediment, and/or changes in the intensity and depth of the oxygen minimum zone. This is recorded in the geochemistry of Cu, Ni, Zn, V, and U, all of which identify interglacial episodes as being more productive.

The detritus of biogenic material promotes active phosphogenesis within the sediments. Both diagenetic enrichment of phosphate and the accumulation of phosphatic skeletal hard parts occurs within the sediments of the Oman Margin and Owen Ridge. Their distribution also reflects the higher productivity of interglacial episodes. This observation that temporal trends in productivity in the northwest Arabian Sea are out of phase with those in the Panama Basin and off northwest Africa, where higher productivity occurs during glacial episodes, will require an answer from integrated studies of ocean productivity and upwelling through time.

ACKNOWLEDGMENTS

We wish to thank staff and crew of the Ocean Drilling Program and the *JOIDES Resolution* for the opportunity to undertake this study. We especially grateful to Warren Prell, Kay Emeis, Brian Price, Tom Pedersen, Dave Murray, and Steve Clemens for helpful discussions on this project. Drs. R. François and H.-J. Brumsack provided critical and stimulating reviews. GBS acknowledges the support of NERC Grant GST/02/315 from the ODP Special Topic fund.

REFERENCES

Adelseck, C. G., Jr., and Anderson, T. F., 1978. The late Pleistocene record of productivity fluctuations in the eastern equatorial Pacific Ocean. *Geology*, 6:388–391.

Baker, P. A., Gieskes, J. M., and Elderfield, H., 1982. Diagenesis of carbonates in deep-sea sediments: evidence from Sr^{2+}/Ca^{2+} ratios and interstitial dissolved Sr^{2+} data. *J. Sediment. Petrol.*, 52:71–82.

Bishop, J.K.B., 1988. The barite-opal organic carbon association in oceanic particulate matter. *Nature*, 332:341–343.

Bonatti, E., Fisher, D. E., Joensuu, O., and Rydell, H. S., 1971. Post-depositional mobility of some transition elements, phosphorus, uranium and thorium in deep-sea sediments. *Geochim. Cosmochim. Acta*, 35:189–201.

Bonatti, E., Simmons, E. C., Berger, D., Hamlyn, P. R., and Lawrence, L., 1983. Ultramafic rock/seawater interaction in the oceanic crust. Mg-silicate (sepiolite) deposit from the Indian Ocean floor. *Earth Planet. Sci. Lett.*, 62:229–238.

Boyle, E. A., 1983. Chemical accumulation variations under the Peru Current during the past 130,000 years. *J. Geophys. Res.*, 88:7667–7680.

_____, 1986. Paired carbon isotope and cadmium data from benthic foraminifera: implications for changes in oceanic phosphorus, oceanic circulation, and atmospheric carbon dioxide. *Geochim. Cosmochim. Acta*, 50:265–276.

_____, 1988. The role of vertical chemical fractionation in controlling late Quaternary atmospheric carbon dioxide. *J. Geophys. Res.*, 93:15701–15714.

Boyle, E. A., and Keigwin, L., 1987. North Atlantic thermohaline circulation during the past 20,000 years linked to high-latitude surface temperature. *Nature*, 330:35–40.

Church, T. M., 1979. Marine barite. *In* Burns, R. G. (Ed.), *Reviews in Mineralogy* (Vol. 6). Mineral Soc. Am., 175–209.

CLIMAP Project Members, 1976. The surface of the ice-age Earth. *Science*, 191:1131–1137.

Duplessy J. C., Shackleton, N. J., Fairbanks, R. G., Labeyrie, L., Oppo, D., and Kallel, N., 1988. Deepwater source variations during the last climatic cycle and their impact on global deepwater circulation. *Paleoceanography*, 3:343–360.

Dymond, J., 1981. Geochemistry of Nazca plate surface sediments: An evaluation of hydrothermal, biogenic, detrital, and hydrogenous sources. *Mem. Geol. Soc. Am.*, 154:133–173.

Fenchel, T., and Finlay, B. J., 1984. Geotaxis in the ciliated protozoan, Loxodes. *J. Exp. Biol.*, 110:17–33.

Finlay, B. J., Hetherington, N. B., and Davison, W., 1983. Active biological participation in lacustrine barium geochemistry. *Geochim. Cosmochim. Acta*, 47:1325–1329.

Finney, B. P., Lyle, M. W., and Heath, G. R., 1988. Sedimentation at MANOP Site H (eastern equatorial Pacific) over the past 400,000 years: climatically induced redox variations and their effects on transition metal cycling. *Paleoceanography*, 3:169–189.

Imbrie, J., Hays, J. D., Martinson, D. G., McIntyre, A., Mix, A. C., Morley, J. J., Pisias, N. G., Prell, W. L., and Shackleton, N. J., 1984. The orbital theory of Pleistocene climate: support from a revised chronology of the marine delta $\delta^{18}O$ record. *In* Berger, A., Imbrie, J., Hays, J., Kukla, G., and Saltzman, B. (Eds.), *Milankovitch and Climate* (Pt. 1): Dordrecht (D. Reidel), 269–305.

Jickells, T. D., Deuser, W. G., and Knap, A. H., 1984. The sedimentation rates of trace elements in the Sargasso Sea measured by sediment trao. *Deep-Sea Res. Part A*, 31:1169–1178.

Keir, R. S., 1988. On the late Pleistocene ocean geochemistry and circulation. *Paleoceanography*, 3:413–445.

Kolla, V., Ray, P. K., and Kostecki, J. A., 1981. Surficial sediments of the Arabian Sea. *Mar. Geol.*, 41:183–204.

Labracherie, M., Barde, M.-F., Moyes, J., and Pujos-Lamy, A., 1983. Variability of upwelling regimes (northwest Africa, south Arabia) during the latest Pleistocene: a comparison. *In* Suess, E., and Thiede, J. (Eds.), *Coastal Upwelling, Its Sediment Record*: New York (Plenum), 347–364.

Lea, D., and Boyle, E. A., 1989. Barium content of benthic foraminifera controlled by bottom-water composition. *Nature*, 338:751–753.

Lea, D. W., Shen, G. T., and Boyle, E. A., 1989. Coralline barium records temporal variability in equatorial Pacific upwelling. *Nature*, 340:373–376.

Li, Y.-H., 1982. Interelement relationship in abyssal Pacific ferromanganese nodules and associated pelagic sediments. *Geochim. Cosmochim. Acta*, 46:1053–1060.

Lyle, M., Heath, G. R., Murray, D. W., Finney, B. P., Dymond, J., Robbins, J. M., and Brooksforce, K., 1988. The record of late Pleistocene sedimentation in the eastern equatorial Pacific Ocean. *Paleoceanography*, 3:39–59.

McMurtry, G. M., and Yeh, H. W., 1981. Hydrothermal clay mineral formation of East Pacific Rise and Bauer Basin sediments. *Chem. Geol.*, 32:189–205.

Moseley, F., and Abbotts, I. L., 1979. The Ophiolite mélange of Masirah, Oman. *J. Geol. Soc. London*, 136:713–724.

Nath, B. G., Rao, V. P., and Becker, K. P., 1989. Geochemical evidence of terrigenous influence in deep-sea sediments up to 8°S in the central Indian basin. *Mar. Geol.*, 87:301–313.

Norrish, K., and Hutton, J. T., 1969. An accurate X-ray spectrographic method for the analysis of a wide range of geological samples. *Geochim. Cosmochim. Acta*, 33:431–453.

Pedersen, T. F., 1983. Increased productivity in the eastern equatorial Pacific during the last glacial maximum (19,000 to 14,000 yr B.P.). *Geology*, 11:16–19.

Pedersen, T. F., Pickering, M., Vogel J. S., Southon, J. N., and Nelson, D. E., 1988. The response of benthic foraminifera to productivity cycles in the eastern equatorial Pacific: faunal and geochemical constraints on glacial bottom water oxygen levels. *Paleoceanography*, 3: 157–168.

Prell, W. L., 1984a. Monsoonal climate of the Arabian Sea during the late Quaternary: a response to changing solar radiation. *In* Berger, A. L., Imbrie, J., Hays, J., Kukla, G., and Saltzman, B. (Eds.). *Milankovitch and Climate* (Pt. 1): Dordrecht (D. Reidel), 349–366.

_____, 1984B. Variation of monsoonal upwelling: a response to changing solar radiation. *In* Hansen, J. E., and Takahashi, T. (Eds.), *Climatic Processes and Climate Sensitivity.* Am. Geophys. Union, Maurice Ewing Ser., 5:48–57.

Prell, W. L., and Kutzbach, J. E., 1987. Monsoon variability over the past 150,000 years. *J. Geophys. Res.*, 92:8411–8425.

Prell, W. L., and Van Campo, E., 1986. Coherent response of Arabian Sea upwelling and pollen transport to late Quaternary monsoonal winds. *Nature*, 323:526–528.

Quasim, S. Z., 1982. Oceanography of the northern Arabian Sea. *Deep-Sea Res. Part A*, 29:1041–1068.

Rao, D. P., and Jayaramna, R., 1970. On the occurrence of oxygen maxima and minima in the upper 500 meters of the north-west Indian Ocean. *Proc. Indian Acad. Sci.*, 71B:230–246.

Revelle, R., Bramlette, M., Arrhenius, G., and Goldberg, E. D., 1955. Pelagic sediments of the Pacific. *Spec. Pap.—Geol. Soc. Am.*, 62: 221–235.

Schmitz, B., 1987. The TiO_2/Al_2O_3 ratio in the Cenozoic Bengal Abyssal Fan sediments and its use as a paleostream energy indicator. *Mar. Geol.*, 76:195–206.

Sen Gupta, R., Fondekar, S. P., Sankaranarayanan, V. E., and De Sousa, S. N., 1975. Chemical oceanography of the Arabian Sea. Part 1. Hydrochemical and hydrographical features of the northern basin. *Indian J. Mar. Sci.*, 4:136–140.

Shankar, R., Subbarao, K. V., and Kolla, V., 1987. Geochemistry of surface sediments from the Arabian Sea. *Mar. Geol.*, 76:253–279.

Shimmield, G. B., 1985. The geochemistry and mineralogy of Pacific sediments, Baja California, Mexico [Ph.D. dissert.]. Univ. of Edinburgh, Edinburgh.

Shimmield, G. B., Price, N. B., and Pedersen, T. F., 1990. The influence of hydrography, bathymetry, and productivity on sediment type and composition from the Oman margin and the northwest Arabian Sea. *In* Robertson, A.H.F., Searle, M. P., and Ries, A. C. (Eds.), *The Geology and Tectonics of the Oman Region.* Spec. Publ. Geol. Soc., 49:761–771.

Shipboard Scientific Party, 1989a. Site 722. *In* Prell, W. L., Niitsuma, N., et al., *Proc. ODP, Init. Repts.*, 117: College Station, TX (Ocean Drilling Program), 255–318.

_____, 1989b. Site 724. *In* Prell, W. L., Niitsuma, N., et al., *Proc. ODP, Init. Repts.*, 117: College Station, TX (Ocean Drilling Program), 385–418.

Sirocko, F., and Sarnthein, M., 1989. Wind-borne deposits in the northwest Indian Ocean: record of Holocene sediments versus modern satellite data. *In* Leinen, M., and Sarnthein, M. (Eds.), *Paleoclimatology and Paleometeorology: Modern and Past Patterns of Global Atmospheric Transport.* NATO ASI Ser., 401–433.

Slater, R. D., and Kroopnick, P., 1984. Controls on dissolved oxygen distribution and organic carbon deposition in the Arabian Sea. *In* Haq, B. U., and Milliman, J. D. (Eds.), *Marine Geology and Oceanography of Arabian Sea and Coastal Pakistan.* New York (Van Nostrand Reinhold), 305–313.

Spears, D. A., and Kanaris-Sotiriou, R., 1976. Titanium in some Carboniferous sediments from Great Britain. *Geochim. Cosmochim. Acta*, 40:345–351.

Thomson, J., Colley, S., Higgs, N., Hydes, D. J., Wilson, T.R.S., and Sørensen, J., 1987. Geochemical oxidation fronts in NE Atlantic distal turbidites and their effects on the sedimentary record. *In* Weaver, P.P.E., and Thomson, J. (Eds.), *Geology and Geochemistry of Abyssal Plains*, Spec. Publ. Geol. Soc., 31:167–178.

Turekian, K. K., and Wedepohl, K. H., 1961. Distribution of the elements in some major units of the earth's crust. *Geol. Soc. Am. Bull.*, 72:175–192.

Van Campo, E., Duplessy, J. C., and Rossignol-Strict, M., 1982. Climatic conditions deduced from a 150-kyr oxygen isotope-pollen record from the Arabian Sea. *Nature*, 296:56–59.

Date of initial receipt: 28 September 1989
Date of acceptance: 20 July 1990
Ms 117B-170

APPENDIX A

Hole 722B Cores 1H and 2H Corrected for Salt Contribution and Dilution.

Sample identification	Depth (mbsf)	Density (g/cm^3)	[a]Age (k.y.)	Si (wt%)	Al (wt%)	Fe (wt%)	Ca (wt%)	Ti (wt%)	Mn (wt%)	P (wt%)
722B-1H-01, 06–08 cm	0.07	0.77	6.0	6.176	1.409	0.890	30.311	0.095	0.018	0.041
722B-1H-01, 16–18 cm	0.17	0.79	7.5	4.748	1.111	0.723	32.318	0.073	0.019	0.035
722B-1H-01, 26–28 cm	0.27	0.87	9.0	4.555	1.111	0.732	32.283	0.071	0.018	0.034
722B-1H-01, 36–38 cm	0.37	0.91	10.2	7.418	1.973	1.240	28.648	0.135	0.025	0.042
722B-1H-01, 46–48 cm	0.47	0.87	11.5	6.009	1.578	1.006	30.306	0.109	0.019	0.037
722B-1H-01, 56–58 cm	0.57	0.93	12.8	8.077	2.115	1.312	27.246	0.147	0.027	0.045
722B-1H-01, 66–68 cm	0.67	0.97	14.0	8.673	2.219	1.322	26.661	0.153	0.024	0.046
722B-1H-01, 76–78 cm	0.77	0.97	15.0	9.260	2.340	1.426	25.705	0.168	0.029	0.049
722B-1H-01, 86–88 cm	0.87	1.00	16.1	10.223	2.687	1.636	24.741	0.187	0.034	0.047
722B-1H-01, 96–98 cm	0.97	0.96	17.2	9.373	2.389	1.464	25.454	0.172	0.028	0.049
722B-1H-01, 106–108 cm	1.07	0.95	19.2	9.145	2.344	1.507	26.074	0.166	0.025	0.052
722B-1H-01, 116–118 cm	1.17	0.97	21.2	9.035	2.312	1.448	26.053	0.166	0.026	0.049
722B-1H-01, 126–128 cm	1.27	1.02	22.3	9.646	2.447	1.554	25.561	0.172	0.028	0.047
722B-1H-01, 136–138 cm	1.37	0.95	25.5	9.038	2.327	1.437	26.202	0.166	0.029	0.051
722B-1H-01, 146–148 cm	1.47	0.97	27.7	9.197	2.335	1.465	26.123	0.168	0.026	0.052
722B-1H-02, 06–08 cm	1.57	1.04	29.8	10.188	2.603	1.592	24.611	0.185	0.026	0.052
722B-1H-02, 16–18 cm	1.67	0.94	31.9	9.358	2.371	1.489	25.634	0.172	0.027	0.054
722B-1H-02, 26–28 cm	1.77	1.01	34.0	9.008	2.273	1.407	26.590	0.164	0.027	0.052
722B-1H-02, 36–38 cm	1.87	0.94	36.0	9.166	2.365	1.445	26.229	0.167	0.025	0.053
722B-1H-02, 46–48 cm	1.97	1.00	38.1	9.952	2.606	1.474	24.132	0.184	0.031	0.049
722B-1H-02, 56–58 cm	2.07	0.88	40.1	7.691	1.983	1.201	28.251	0.145	0.024	0.052
722B-1H-02, 66–68 cm	2.17	0.84	42.1	8.039	1.883	1.191	27.894	0.141	0.024	0.046
722B-1H-02, 76–78 cm	2.27	0.83	44.1	8.963	2.036	1.265	26.595	0.153	0.025	0.052
722B-1H-02, 86–88 cm	2.37	1.07	46.2	9.246	2.014	1.401	25.506	0.145	0.022	0.052
722B-1H-02, 96–98 cm	2.47	0.94	48.2	8.862	2.251	1.368	26.271	0.163	0.025	0.054
722B-1H-02, 106–108 cm	2.57	0.89	50.3	7.690	1.828	1.180	28.143	0.133	0.021	0.058
722B-1H-02, 116–118 cm	2.67	0.92	52.3	8.019	1.756	1.137	28.115	0.127	0.021	0.052
722B-1H-02, 126–128 cm	2.77	0.96	54.3	7.820	1.911	1.183	27.309	0.134	0.025	0.045
722B-1H-02, 136–138 cm	2.87	0.94	56.3	7.496	1.892	1.178	26.861	0.131	0.020	0.041
722B-1H-02, 146–148 cm	2.97	0.90	58.4	7.207	1.730	1.116	28.918	0.124	0.023	0.046
722B-1H-03, 06–08 cm	3.07	1.00	60.4	9.369	2.401	1.460	26.046	0.171	0.026	0.046
722B-1H-03, 16–18 cm	3.17	1.10	62.5	12.217	3.134	1.896	23.770	0.222	0.032	0.050
722B-1H-03, 26–28 cm	3.27	1.00	65.1	11.010	2.834	1.674	24.167	0.204	0.030	0.049
722B-1H-03, 36–38 cm	3.37	1.10	67.7	10.109	2.607	1.574	25.258	0.188	0.029	0.049
722B-1H-03, 46–48 cm	3.47	1.14	70.1	10.728	2.736	1.672	23.040	0.203	0.028	0.052
722B-1H-03, 56–58 cm	3.57	1.08	73.2	10.178	2.678	1.606	24.667	0.181	0.025	0.050
722B-1H-03, 66–68 cm	3.67	1.03	76.2	7.867	2.009	1.230	28.328	0.144	0.026	0.050
722B-1H-03, 76–78 cm	3.77	0.99	79.2	6.604	1.670	1.097	29.959	0.118	0.022	0.054
722B-1H-03, 86–88 cm	3.87	1.07	84.1	8.720	2.308	1.514	27.048	0.161	0.026	0.052
722B-1H-03, 96–98 cm	3.97	1.05	89.0	7.838	2.065	1.283	26.850	0.140	0.021	0.051
722B-1H-03, 106–108 cm	4.07	0.95	93.5	7.680	1.913	3.130	27.679	0.146	0.034	0.048
722B-1H-03, 116–118 cm	4.17	0.93	98.0	6.974	1.600	1.044	29.472	0.117	0.024	0.044
722B-1H-03, 126–128 cm	4.27	1.07	103.2	7.667	2.019	1.231	28.841	0.139	0.022	0.051
722B-1H-03, 136–138 cm	4.37	1.07	107.5	7.035	1.890	1.161	29.304	0.127	0.020	0.042
722B-1H-03, 146–148 cm	4.47	0.96	113.1	6.109	1.466	0.970	30.622	0.103	0.021	0.046
722B-1H-04, 06–08 cm	4.57	1.04	116.8	8.802	2.347	1.479	26.922	0.161	0.025	0.048
722B-1H-04, 16–18 cm	4.67	0.96	119.8	7.644	1.927	1.188	28.259	0.128	0.026	0.048
722B-1H-04, 26–28 cm	4.77	0.98	122.8	6.105	1.552	1.009	30.683	0.099	0.023	0.040
722B-1H-04, 36–38 cm	4.87	0.86	124.1	5.635	1.411	0.911	31.310	0.093	0.025	0.040
722B-1H-04, 46–48 cm	4.97	1.07	126.0	9.234	2.466	1.429	26.062	0.168	0.028	0.051
722B-1H-04, 56–58 cm	5.07	1.05	127.5	9.281	2.456	1.499	25.765	0.169	0.029	0.052
722B-1H-04, 66–68 cm	5.17	1.11	129.2	9.206	2.382	1.416	26.319	0.165	0.032	0.056
722B-1H-04, 76–78 cm	5.27	1.01	132.0	9.444	2.452	1.499	25.551	0.171	0.029	0.058
722B-2H-01, 06–08 cm	5.62	0.93	135.8	8.235	2.123	1.505	26.966	0.149	0.023	0.051
722B-2H-01, 16–18 cm	5.67	1.00	137.1	8.436	2.145	1.419	26.834	0.151	0.027	0.050
722B-2H-01, 26–28 cm	5.77	1.04	138.2	8.978	2.265	1.417	26.477	0.158	0.027	0.051
722B-2H-01, 36–38 cm	5.87	0.89	140.5	9.584	2.442	1.437	26.022	0.170	0.030	0.048
722B-2H-01, 46–48 cm	5.97	1.06	142.6	9.425	2.386	1.499	25.491	0.166	0.030	0.055
722B-2H-01, 56–58 cm	6.07	1.10	144.1	9.355	2.402	1.597	25.643	0.167	0.030	0.050
722B-2H-01, 66–68 cm	6.17	1.25	145.2	9.100	2.339	1.746	25.810	0.162	0.030	0.067
722B-2H-01, 76–78 cm	6.27	1.24	147.6	11.982	3.059	1.832	22.246	0.215	0.036	0.047
722B-2H-01, 86–88 cm	6.37	1.20	149.4	12.599	3.202	1.913	21.618	0.231	0.036	0.049
722B-2H-01, 96–98 cm	6.47	1.14	151.2	11.323	2.850	1.779	23.430	0.206	0.034	0.053
722B-2H-01, 106–108 cm	6.57	1.06	152.7	11.650	2.935	1.865	22.789	0.212	0.034	0.052
722B-2H-01, 116–118 cm	6.67	1.10	154.2	11.879	3.029	1.838	22.713	0.219	0.033	0.054
722B-2H-01, 126–128 cm	6.77	1.14	156.2	12.557	3.210	1.968	21.598	0.226	0.037	0.051
722B-2H-01, 136–138 cm	6.87	1.10	158.0	11.813	3.052	1.919	22.128	0.216	0.033	0.054
722B-2H-01, 146–148 cm	6.97	1.16	159.5	12.613	3.284	1.933	21.397	0.227	0.034	0.051
722B-2H-01, 06–08 cm	7.07	1.05	161.4	11.021	2.834	1.679	23.490	0.201	0.029	0.055
722B-2H-01, 16–18 cm	7.17	1.01	163.2	10.031	2.578	1.652	25.032	0.178	0.031	0.050
722B-2H-02, 26–28 cm	7.27	1.21	165.0	10.247	2.625	1.646	24.408	0.179	0.029	0.047
722B-2H-02, 36–38 cm	7.37	1.06	166.8	9.493	2.487	1.469	25.905	0.170	0.031	0.045
722B-2H-02, 46–48 cm	7.47	1.07	168.7	10.192	2.704	1.618	24.731	0.185	0.027	0.044
722B-2H-02, 56–58 cm	7.57	1.11	170.7	10.105	2.658	1.726	24.793	0.185	0.032	0.046
722B-2H-02, 66–68 cm	7.67	1.08	172.8	10.088	2.656	1.717	24.971	0.187	0.030	0.047

Appendix A (continued).

Sample identification	Depth (mbsf)	Density (g/cm^3)	[a]Age (k.y.)	Si (wt%)	Al (wt%)	Fe (wt%)	Ca (wt%)	Ti (wt%)	Mn (wt%)	P (wt%)
722B-2H-02, 76–78 cm	7.77	1.12	175.2	8.916	2.178	1.445	26.709	0.177	0.027	0.041
722B-2H-02, 86–88 cm	7.87	1.10	177.6	9.970	2.604	1.629	25.216	0.188	0.031	0.049
722B-2H-02, 96–98 cm	7.97	1.13	180.0	10.263	2.666	1.715	24.421	0.194	0.031	0.050
722B-2H-02, 106–108 cm	8.07	1.07	182.0	10.180	2.567	1.541	25.041	0.183	0.025	0.047
722B-2H-02, 116–118 cm	8.17	1.01	184.1	10.153	2.481	1.564	25.294	0.177	0.027	0.045
722B-2H-02, 126–128 cm	8.27	1.06	186.2	6.843	1.839	1.119	29.875	0.120	0.023	0.042
722B-2H-02, 136–138 cm	8.37	1.04	187.7	6.551	1.735	1.019	30.032	0.116	0.022	0.042
722B-2H-02, 146–148 cm	8.47	1.01	189.7	5.799	1.502	0.977	30.898	0.102	0.021	0.041
722B-2H-03, 06–08 cm	8.57	0.98	191.1	6.378	1.599	1.015	30.506	0.111	0.023	0.046
722B-2H-03, 16–18 cm	8.67	0.97	193.2	6.334	1.507	0.928	30.703	0.109	0.023	0.043
722B-2H-03, 26–28 cm	8.77	0.90	197.6	7.165	1.549	0.961	29.884	0.108	0.025	0.044
722B-2H-03, 36–38 cm	8.87	1.01	200.8	5.617	1.176	0.762	31.585	0.081	0.022	0.040
722B-2H-03, 46–48 cm	8.97	0.88	204.3	5.346	1.159	0.731	32.241	0.077	0.025	0.043
722B-2H-03, 56–58 cm	9.07	0.99	208.0	7.199	1.868	1.194	29.634	0.122	0.027	0.046
722B-2H-03, 66–68 cm	9.17	1.07	211.5	7.961	2.340	1.353	26.396	0.162	0.026	0.047
722B-2H-03, 76–78 cm	9.27	1.16	215.0	10.700	2.809	1.651	22.998	0.192	0.032	0.046
722B-2H-03, 86–88 cm	9.37	1.14	218.5	10.118	2.714	1.565	26.356	0.189	0.029	0.050
722B-2H-03, 96–98 cm	9.47	1.05	222.1	8.080	2.175	1.393	29.185	0.160	0.030	0.053
722B-2H-03, 106–108 cm	9.57	1.06	225.8	7.968	2.152	1.466	27.398	0.150	0.027	0.050
722B-2H-03, 116–118 cm	9.67	1.13	229.8	8.684	2.362	1.598	25.956	0.162	0.030	0.048
722B-2H-03, 126–128 cm	9.77	1.08	233.4	7.694	2.006	1.190	30.153	0.140	0.025	0.049
722B-2H-03, 136–138 cm	9.87	1.05	237.0	6.425	1.623	0.999	31.277	0.111	0.023	0.049
722B-2H-03, 146–148 cm	9.97	1.02	239.0	5.256	1.315	0.815	32.903	0.087	0.023	0.046
722B-2H-04, 06–08 cm	10.07	0.98	241.0	8.154	2.145	1.476	24.239	0.148	0.026	0.044
722B-2H-04, 16–18 cm	10.17	0.95	242.9	7.109	1.865	1.170	29.505	0.122	0.023	0.045
722B-2H-04, 26–28 cm	10.27	0.98	244.8	7.938	2.055	1.276	29.448	0.146	0.028	0.053
722B-2H-04, 36–38 cm	10.37	1.04	246.3	9.253	2.415	1.366	24.736	0.166	0.029	0.047
722B-2H-04, 46–48 cm	10.47	0.99	248.1	8.264	2.081	1.316	26.525	0.153	0.026	0.053
722B-2H-04, 56–58 cm	10.57	0.97	249.8	8.231	2.069	1.292	27.337	0.149	0.025	0.052
722B-2H-04, 66–68 cm	10.67	0.99	251.7	8.071	1.983	1.247	27.731	0.143	0.025	0.050
722B-2H-04, 76–78 cm	10.77	0.91	253.2	7.864	1.617	1.034	28.682	0.115	0.022	0.045
722B-2H-04, 86–88 cm	10.87	0.90	255.0	8.507	1.620	1.047	28.061	0.115	0.023	0.045
722B-2H-04, 96–98 cm	10.97	0.93	256.6	8.500	1.994	1.233	27.551	0.138	0.027	0.044
722B-2H-04, 106–108 cm	11.07	1.02	258.2	8.887	2.096	1.218	27.008	0.150	0.027	0.048
722B-2H-04, 116–118 cm	11.17	1.02	259.8	8.834	2.094	1.253	26.834	0.148	0.027	0.046
722B-2H-04, 126–128 cm	11.27	1.16	261.6	10.604	2.711	1.631	25.144	0.188	0.036	0.047
722B-2H-04, 136–138 cm	11.37	1.16	263.2	10.683	2.762	1.727	25.039	0.189	0.032	0.046
722B-2H-04, 146–148 cm	11.47	1.19	265.0	11.420	3.004	1.675	23.859	0.206	0.031	0.049
722B-2H-05, 06–08 cm	11.57	1.39	266.5	10.758	2.723	1.664	24.551	0.194	0.033	0.052
722B-2H-05, 16–18 cm	11.67	1.20	268.0	10.239	2.644	1.540	25.277	0.186	0.030	0.056
722B-2H-05, 26–28 cm	11.77	1.14	271.5	9.652	2.471	1.558	26.132	0.180	0.026	0.049
722B-2H-05, 36–38 cm	11.87	1.14	277.0	10.505	2.728	1.620	24.207	0.194	0.029	0.054
722B-2H-05, 46–48 cm	11.97	1.03	281.5	6.963	1.654	1.052	29.662	0.116	0.022	0.043
722B-2H-05, 56–58 cm	12.07	1.07	286.0	4.899	1.207	0.748	32.520	0.079	0.020	0.037
722B-2H-05, 66–68 cm	12.17	1.07	289.0	5.587	1.478	0.865	31.766	0.100	0.021	0.039
722B-2H-05, 76–78 cm	12.27	1.1	292.0	5.445	1.453	0.902	31.812	0.101	0.022	0.042
722B-2H-05, 86–88 cm	12.37	1.12	295.0	5.758	1.529	0.997	30.904	0.108	0.021	0.040
722B-2H-05, 96–98 cm	12.47	1.09	298.0	6.451	1.646	1.067	30.024	0.123	0.024	0.044
722B-2H-05, 106–108 cm	12.57	1.09	302.0	5.929	1.522	0.916	30.899	0.110	0.021	0.042
722B-2H-05, 116–118 cm	12.67	1.01	306.0	5.230	1.358	0.849	32.940	0.093	0.023	0.044
722B-2H-05, 126–128 cm	12.77	1.05	310.0	6.533	1.489	0.955	29.403	0.106	0.020	0.039
722B-2H-05, 136–138 cm	12.87	1.10	314.0	4.479	1.121	0.700	32.847	0.076	0.017	0.041
722B-2H-05, 146–148 cm	12.97	1.12	318.0	5.365	1.424	0.853	31.943	0.095	0.018	0.046
722B-2H-06, 06–08 cm	13.07	1.06	322.0	5.795	1.543	0.969	31.263	0.107	0.020	0.053
722B-2H-06, 16–18 cm	13.17	1.03	326.0	5.048	1.242	0.780	32.510	0.087	0.020	0.050
722B-2H-06, 26–28 cm	13.27	0.98	330.0	5.453	1.165	0.748	32.112	0.083	0.020	0.043
722B-2H-06, 36–38 cm	13.37	1.01	331.5	4.718	1.156	0.709	32.903	0.076	0.018	0.042
722B-2H-06, 46–48 cm	13.47	1.02	333.1	5.170	1.362	0.828	32.301	0.086	0.021	0.049
722B-2H-06, 56–58 cm	13.57	1.06	334.6	6.000	1.553	0.992	30.762	0.103	0.024	0.043
722B-2H-06, 66–68 cm	13.67	1.10	336.1	6.082	1.643	0.991	30.533	0.113	0.027	0.042
722B-2H-06, 76–78 cm	13.77	1.10	337.6	6.833	1.837	1.240	28.810	0.126	0.028	0.044
722B-2H-06, 86–88 cm	13.87	1.11	338.8	6.961	1.840	1.119	29.125	0.126	0.028	0.044
722B-2H-06, 96–98 cm	13.97	1.12	340.8	8.844	2.302	1.347	30.093	0.160	0.032	0.052
722B-2H-06, 106–108 cm	14.07	0.94	342.8	8.108	2.113	1.207	28.116	0.148	0.026	0.047
722B-2H-06, 116–118 cm	14.17	1.05	344.8	7.586	1.939	1.211	28.292	0.140	0.027	0.057
722B-2H-06, 126–128 cm	14.27	1.10	347.0	7.960	2.028	1.199	28.049	0.146	0.027	0.054
722B-2H-06, 136–138 cm	14.37	1.05	349.2	7.488	1.849	1.204	28.465	0.134	0.026	0.048
722B-2H-06, 146–148 cm	14.47	1.05	351.6	7.524	1.905	1.205	28.725	0.135	0.024	0.049
722B-2H-07, 06–08 cm	14.57	1.07	353.7	7.839	1.982	1.287	28.236	0.139	0.024	0.055
722B-2H-07, 16–18 cm	14.67	1.07	356.0	7.887	2.043	1.153	28.200	0.140	0.025	0.043
722B-2H-07, 26–28 cm	14.77	1.12	360.5	8.767	2.278	1.475	27.057	0.155	0.030	0.043
722B-2H-07, 36–38 cm	14.87	1.11	365.0	8.573	2.212	1.252	27.747	0.153	0.027	0.042

[a] Chronostratigraphy from Clemens and Prell, pers. comm., March 1989.

APPENDIX B

Hole 722B Cores 1H and 2H Corrected for Salt Contribution and Dilution.

Sample identification	Depth (mbsf)	[a]Age (k.y.)	Ni (ppm)	Cr (ppm)	V (ppm)	Cu (ppm)	Zn (ppm)	Sr (ppm)	Rb (ppm)	Zr (ppm)	Ba (ppm)	Ce (ppm)	Nd (ppm)	Y (ppm)	U (ppm)	Th (ppm)
722B-1H-01, 06–08 cm	0.07	6.0	38	39	37	24	38	1160	16	44	754	18	21	13	4.13	1.37
722B-1H-01, 16–18 cm	0.17	7.5	36	30	39	22	34	1218	13	36	799	8	9	12	—	—
722B-1H-01, 26–28 cm	0.27	9.0	33	40	41	25	32	1205	13	34	693	20	12	11	3.60	2.25
722B-1H-01, 36–38 cm	0.37	10.2	48	59	51	21	40	1114	23	53	325	17	11	14	—	—
722B-1H-01, 46–48 cm	0.47	11.5	39	50	37	24	33	1112	19	46	309	13	14	12	2.55	2.25
722B-1H-01, 56–58 cm	0.57	12.8	52	79	49	20	39	1043	26	57	286	22	11	13	—	—
722B-1H-01, 66–68 cm	0.67	14.0	57	86	51	20	42	960	28	65	295	25	15	15	3.88	2.36
722B-1H-01, 76–78 cm	0.77	15.0	62	91	56	22	49	932	28	68	306	23	14	15	—	—
722B-1H-01, 86–88 cm	0.87	16.1	62	99	63	25	48	948	33	73	224	29	18	15	4.21	2.56
722B-1H-01, 96–98 cm	0.97	17.2	61	99	52	24	45	926	29	67	304	21	17	15	3.18	2.34
722B-1H-01, 106–108 cm	1.07	19.2	76	92	54	41	62	942	29	68	283	26	16	15	3.56	2.50
722B-1H-01, 116–118 cm	1.17	21.2	59	99	52	21	42	964	28	68	254	25	18	13	2.55	2.48
722B-1H-01, 126–128 cm	1.27	22.3	59	94	57	21	40	937	31	69	237	33	23	15	2.71	2.39
722B-1H-01, 136–138 cm	1.37	25.5	59	87	50	21	47	933	28	63	319	12	16	15	2.60	2.41
722B-1H-01, 146–148 cm	1.47	27.7	57	95	52	20	43	956	29	64	311	26	19	13	2.65	2.72
722B-1H-02, 06–08 cm	1.57	29.8	61	100	60	20	45	896	32	74	283	22	19	16	3.98	2.30
722B-1H-02, 16–18 cm	1.67	31.9	60	90	53	18	46	953	30	70	305	22	13	15	2.89	2.36
722B-1H-02, 26–28 cm	1.77	34.0	55	85	53	20	41	938	29	66	286	23	18	14	2.94	1.57
722B-1H-02, 36–38 cm	1.87	36.0	55	90	52	23	44	962	28	63	321	35	17	14	3.16	2.68
722B-1H-02, 46–48 cm	1.97	38.1	58	96	59	20	43	891	32	70	197	32	20	14	2.90	2.00
722B-1H-02, 56–58 cm	2.07	40.1	48	76	44	24	37	1054	24	58	272	20	17	14	—	—
722B-1H-02, 66–68 cm	2.17	42.1	52	80	43	19	40	1024	22	59	343	20	13	15	3.90	2.04
722B-1H-02, 76–78 cm	2.27	44.1	60	82	47	23	44	1009	25	61	447	25	16	14	3.54	2.33
722B-1H-02, 86–88 cm	2.37	46.2	59	76	46	20	43	988	24	60	450	16	13	13	3.68	2.25
722B-1H-02, 96–98 cm	2.47	48.2	57	90	55	26	43	961	28	64	359	27	19	15	4.10	2.27
722B-1H-02, 106–108 cm	2.57	50.3	52	82	41	23	39	1082	22	55	470	25	20	14	2.96	2.18
722B-1H-02, 116–118 cm	2.67	52.3	51	72	41	23	39	1122	20	53	467	18	12	13	3.00	2.16
722B-1H-02, 126–128 cm	2.77	54.3	48	69	46	17	35	1107	24	54	315	26	14	12	3.26	2.32
722B-1H-02, 136–138 cm	2.87	56.3	48	73	43	17	37	1067	23	52	307	19	11	13	3.20	2.05
722B-1H-02, 146–148 cm	2.97	58.4	47	68	40	21	36	1155	21	52	410	19	20	13	2.77	2.65
722B-1H-03, 06–08 cm	3.07	60.4	58	85	54	21	44	1004	29	65	298	31	19	15	1.73	2.41
722B-1H-03, 16–18 cm	3.17	62.5	71	118	66	22	52	867	39	82	244	33	19	17	2.72	2.83
722B-1H-03, 26–28 cm	3.27	65.1	62	110	64	21	45	874	35	76	251	30	21	17	2.50	2.12
722B-1H-03, 36–38 cm	3.37	67.7	61	110	63	23	43	917	33	73	291	31	21	17	4.74	3.09
722B-1H-03, 46–48 cm	3.47	70.1	77	119	65	22	50	832	33	78	373	22	20	17	3.65	3.46
722B-1H-03, 56–58 cm	3.57	73.2	59	102	55	25	43	907	35	70	296	33	21	17	3.83	2.27
722B-1H-03, 66–68 cm	3.67	76.2	50	74	49	28	40	1064	23	59	372	22	14	15	3.91	1.79
722B-1H-03, 76–78 cm	3.77	79.2	47	63	46	25	35	1082	21	51	441	27	17	14	—	—
722B-1H-03, 86–88 cm	3.87	84.1	53	81	53	23	42	972	28	61	283	21	16	16	3.61	2.39
722B-1H-03, 96–98 cm	3.97	89.0	51	74	50	22	37	977	25	55	372	39	17	15	—	—
722B-1H-03, 106–108 cm	4.07	93.5	—	—	—	—	—	—	—	—	—	—	—	—	3.00	1.80
722B-1H-03, 116–118 cm	4.17	98.0	48	66	46	23	38	1130	19	47	501	21	19	14	3.56	2.34
722B-1H-03, 126–128 cm	4.27	103.2	49	71	51	26	43	1057	25	59	575	26	18	17	—	—
722B-1H-03, 136–138 cm	4.37	107.5	40	51	35	20	33	1144	17	44	492	21	15	14	2.85	1.53
722B-1H-03, 146–148 cm	4.47	113.1	44	71	50	24	38	1103	24	53	419	29	21	16	—	—
722B-1H-04, 06–08 cm	4.57	116.8	59	89	57	28	46	1023	30	64	560	18	14	17	4.77	2.16
722B-1H-04, 16-18 cm	4.67	119.8	55	67	51	27	52	1105	22	55	703	22	19	14	—	—
722B-1H-04, 26–28 cm	4.77	122.8	48	47	51	30	48	1142	20	46	1046	21	15	16	4.45	1.53
722B-1H-04, 36–38 cm	4.87	124.1	44	37	44	25	45	1105	18	42	703	22	16	13	3.34	2.90
722B-1H-04, 46–48 cm	4.97	126.0	55	77	56	22	41	1040	30	65	181	20	16	14	2.71	2.58
722B-1H-04, 56–58 cm	5.07	127.5	61	87	54	19	42	1003	30	63	225	23	18	14	—	—
722B-1H-04, 66–68 cm	5.17	129.2	62	92	54	22	41	1043	28	63	211	20	16	14	3.34	2.28
722B-1H-04, 76–78 cm	5.27	132.0	64	104	57	22	42	980	30	68	249	19	15	15	—	—
722B-2H-01, 06–08 cm	5.62	135.8	60	90	50	20	40	982	26	61	347	34	18	14	3.35	2.34
722B-2H-01, 16–18 cm	5.67	137.1	55	87	56	19	40	978	27	63	336	25	17	14	—	—
722B-2H-01, 26–28 cm	5.77	138.2	56	90	54	21	42	968	28	64	282	21	18	14	2.73	2.43
722B-2H-01, 36–38 cm	5.87	140.5	56	94	59	21	41	939	30	70	275	25	12	15	—	—
722B-2H-01, 46–48 cm	5.97	142.6	56	89	61	20	46	969	30	67	308	30	17	14	2.86	2.31
722B-2H-01, 56–58 cm	6.07	144.1	61	90	61	20	40	944	29	70	233	27	17	15	—	—
722B-2H-01, 66–68 cm	6.17	145.2	71	92	60	19	42	920	29	67	252	28	16	15	2.83	3.45
722B-2H-01, 76–78 cm	6.27	147.6	74	112	76	22	49	784	38	82	203	31	17	17	2.81	3.51
722B-2H-01, 86–88 cm	6.37	149.4	75	125	77	20	51	756	40	88	232	28	15	17	3.06	3.00
722B-2H-01, 96–98 cm	6.47	151.2	72	113	74	19	45	795	34	78	283	41	16	16	3.48	2.98
722B-2H-01, 106–108 cm	6.57	152.7	74	119	77	24	47	755	36	78	317	36	15	15	3.25	2.92
722B-2H-01, 116–118 cm	6.67	154.2	75	123	69	24	52	788	38	82	319	29	18	16	2.69	3.05
722B-2H-01, 126–128 cm	6.77	156.2	80	143	81	22	50	769	41	84	263	40	19	16	3.89	3.02
722B-2H-01, 136–138 cm	6.87	158.0	83	133	66	22	53	802	39	78	350	32	16	15	2.67	3.41
722B-2H-01, 146–148 cm	6.97	159.5	78	133	80	22	52	740	41	86	265	35	15	17	3.31	2.77
722B-2H-02, 06–08 cm	7.07	161.4	72	122	69	24	50	825	35	78	382	30	18	16	—	—
722B-2H-02, 16–18 cm	7.17	163.2	71	107	66	25	47	883	32	70	401	26	15	15	2.75	2.80
722B-2H-02, 26–28 cm	7.27	165.0	66	103	60	23	47	858	32	68	368	29	16	15	3.30	2.40
722B-2H-02, 36–38 cm	7.37	166.8	60	102	59	22	48	940	30	65	399	28	18	15	—	—
722B-2H-02, 46–48 cm	7.47	168.7	67	97	67	20	45	870	33	69	302	23	14	17	3.19	2.70
722B-2H-02, 56–58 cm	7.57	170.7	70	103	67	21	48	866	32	70	354	19	15	16	—	—
722B-2H-02, 66–68 cm	7.67	172.8	64	96	69	19	48	870	32	68	339	26	18	16	2.87	2.52

Appendix B (continued).

Sample identification	Depth (mbsf)	[a]Age (k.y.)	Ni (ppm)	Cr (ppm)	V (ppm)	Cu (ppm)	Zn (ppm)	Sr (ppm)	Rb (ppm)	Zr (ppm)	Ba (ppm)	Ce (ppm)	Nd (ppm)	Y (ppm)	U (ppm)	Th (ppm)
722B-2H-02, 76–78 cm	7.77	175.2	57	127	52	19	40	870	26	94	259	25	17	15	—	—
722B-2H-02, 86–88 cm	7.87	177.6	65	96	69	27	45	931	32	67	359	27	17	16	4.11	3.07
722B-2H-02, 96–98 cm	7.97	180.0	73	121	66	31	52	903	32	74	424	34	14	18	—	—
722B-2H-02, 106–108 cm	8.07	182.0	69	108	63	26	51	934	30	70	518	21	15	17	3.04	2.39
722B-2H-02, 116–118 cm	8.17	184.1	71	97	57	25	49	940	30	68	582	25	19	17	—	—
722B-2H-02, 126–128 cm	8.27	186.2	48	54	53	29	41	1113	23	45	645	29	21	16	2.81	—
722B-2H-02, 136–138 cm	8.37	187.7	42	57	49	26	41	1134	21	44	540	22	16	16	—	—
722B-2H-02, 146–148 cm	8.47	189.7	40	50	48	27	37	1179	20	40	521	14	15	14	2.28	—
722B-2H-03, 06–08 cm	8.57	191.1	44	56	45	24	41	1228	18	44	550	12	17	14	—	—
722B-2H-03, 16–18 cm	8.67	193.2	42	52	44	26	34	1256	19	42	548	25	20	13	2.73	—
722B-2H-03, 26–28 cm	8.77	197.6	47	56	52	22	40	1171	17	46	687	29	18	14	—	—
722B-2H-03, 36–38 cm	8.87	200.8	38	37	39	24	39	1224	14	35	737	15	16	12	3.13	1.27
722B-2H-03, 46–48 cm	8.97	204.3	36	31	38	20	36	1277	13	33	714	6	11	12	—	—
722B-2H-03, 56–58 cm	9.07	208.0	51	59	46	25	42	1167	23	48	446	12	15	13	1.81	2.40
722B-2H-03, 66–68 cm	9.17	211.5	57	77	56	20	41	1003	29	57	281	27	17	13	—	—
722B-2H-03, 76–78 cm	9.27	215.0	62	107	75	25	45	842	36	71	265	25	16	16	3.20	2.70
722B-2H-03, 86–88 cm	9.37	218.5	63	97	77	27	46	1013	34	70	323	20	12	17	—	—
722B-2H-03, 96–98 cm	9.47	222.1	66	82	49	30	45	1162	26	59	516	16	16	16	4.18	2.58
722B-2H-03, 106–108 cm	9.57	225.8	63	81	56	28	43	1121	26	56	380	30	12	15	—	—
722B-2H-03, 116–118 cm	9.67	229.8	69	85	63	25	44	1039	28	59	421	27	18	16	3.62	2.13
722B-2H-03, 126–128 cm	9.77	233.4	51	75	55	25	44	1201	23	55	524	31	18	17	—	—
722B-2H-03, 136–138 cm	9.87	237.0	43	54	43	25	38	1252	19	47	573	20	16	15	2.41	1.37
722B-2H-03, 146–148 cm	9.97	239.0	37	38	36	23	34	1310	15	39	602	17	14	13	—	—
722B-2H-04, 06–08 cm	10.07	241.0	38	55	40	22	33	944	19	39	326	23	12	11	—	—
722B-2H-04, 16–18 cm	10.17	242.9	—	90	55	29	39	1027	30	75	242	19	13	14	—	—
722B-2H-04, 26–28 cm	10.27	244.8	52	78	53	22	43	1105	25	60	417	34	19	14	—	—
722B-2H-04, 36–38 cm	10.37	246.3	53	91	55	18	39	937	30	68	263	28	12	14	—	—
722B-2H-04, 46–48 cm	10.47	248.1	52	87	52	23	40	1020	26	62	379	29	13	13	—	—
722B-2H-04, 56–58 cm	10.57	249.8	52	92	47	22	40	1026	25	62	376	26	15	14	—	—
722B-2H-04, 66–68 cm	10.67	251.7	51	76	52	22	40	1058	24	58	398	16	15	14	—	—
722B-2H-04, 76–78 cm	10.77	253.2	45	63	48	19	35	1117	18	49	450	25	14	13	—	—
722B-2H-04, 86–88 cm	10.87	255.0	43	71	42	19	34	1088	19	54	454	22	16	12	—	—
722B-2H-04, 96–98 cm	10.97	256.6	51	72	52	20	38	1070	25	59	369	16	14	13	—	—
722B-2H-04, 106–108 cm	11.07	258.2	51	82	54	20	40	1080	26	60	402	25	14	13	—	—
722B-2H-04, 116–118 cm	11.17	259.8	54	74	53	21	41	1067	26	62	375	23	17	13	—	—
722B-2H-04, 126–128 cm	11.27	261.6	60	95	59	20	42	977	34	73	262	39	15	15	—	—
722B-2H-04, 136–138 cm	11.37	263.2	64	92	64	19	46	981	35	75	209	27	16	17	—	—
722B-2H-04, 146–148 cm	11.47	265.0	61	89	67	21	45	954	34	76	259	24	16	17	—	—
722B-2H-05, 06–08 cm	11.57	266.5	63	99	80	25	46	948	35	77	356	15	18	17	—	—
722B-2H-05, 16–18 cm	11.67	268.0	61	102	66	23	48	991	32	73	364	23	16	18	—	—
722B-2H-05, 26–28 cm	11.77	271.5	66	111	72	26	49	987	36	80	330	29	15	19	—	—
722B-2H-05, 36–38 cm	11.87	277.0	65	94	61	21	42	987	28	77	383	20	17	15	—	—
722B-2H-05, 46–48 cm	11.97	281.5	45	57	49	23	40	1227	19	61	514	23	21	14	—	—
722B-2H-05, 56–58 cm	12.07	286.0	31	30	37	24	32	1442	14	43	498	21	20	13	—	—
722B-2H-05, 66–68 cm	12.17	289.0	33	41	39	22	31	1359	18	49	242	22	15	13	—	—
722B-2H-05, 76–78 cm	12.27	292.0	37	44	47	21	29	1364	17	49	348	11	15	14	—	—
722B-2H-05, 86–88 cm	12.37	295.0	39	53	43	22	28	1333	18	54	253	12	13	15	—	—
722B-2H-05, 96–98 cm	12.47	298.0	51	76	39	26	36	1255	19	60	493	10	8	15	—	—
722B-2H-05, 106–108 cm	12.57	302.0	42	63	49	27	37	1348	17	55	439	19	11	12	—	—
722B-2H-05, 116–118 cm	12.67	306.0	44	59	41	28	37	1398	18	60	605	18	12	14	—	—
722B-2H-05, 126–128 cm	12.77	310.0	38	39	33	21	27	1335	14	48	383	21	17	13	—	—
722B-2H-05, 136–138 cm	12.87	314.0	34	33	33	21	28	1424	13	48	368	22	16	13	—	—
722B-2H-05, 146–148 cm	12.97	318.0	32	37	42	26	31	1352	16	53	425	20	16	15	—	—
722B-2H-06, 06–08 cm	13.07	322.0	37	48	47	25	34	1340	19	56	391	12	7	15	—	—
722B-2H-06, 16–18 cm	13.17	326.0	33	40	38	27	29	1431	14	52	524	14	16	13	—	—
722B-2H-06, 26–28 cm	13.27	330.0	35	40	33	20	27	1441	12	51	502	6	11	12	—	—
722B-2H-06, 36–38 cm	13.37	331.5	32	35	35	21	36	1489	12	49	582	12	12	12	—	—
722B-2H-06, 46–48 cm	13.47	333.1	32	40	31	24	30	1381	15	53	449	25	18	14	—	—
722B-2H-06, 56–58 cm	13.57	334.6	39	48	36	23	35	1283	19	56	301	18	18	12	—	—
722B-2H-06, 66–68 cm	13.67	336.1	37	52	37	17	25	1364	19	58	120	17	19	10	—	—
722B-2H-06, 76–78 cm	13.77	337.6	45	59	40	20	29	1266	22	63	118	26	13	11	—	—
722B-2H-06, 86–88 cm	13.87	338.8	41	64	41	15	27	1271	22	62	183	17	11	12	—	—
722B-2H-06, 96–98 cm	13.97	340.8	50	95	51	25	38	1245	28	75	186	17	15	14	—	—
722B-2H-06, 106–108 cm	14.07	342.8	59	71	51	17	35	1183	26	71	222	31	16	14	—	—
722B-2H-06, 116–118 cm	14.17	344.8	49	81	50	21	41	1140	23	69	334	16	15	15	—	—
722B-2H-06, 126–128 cm	14.27	347.0	46	75	46	19	35	1149	25	73	319	20	11	14	—	—
722B-2H-06, 136–138 cm	14.37	349.2	46	71	47	21	33	1166	22	68	351	24	13	14	—	—
722B-2H-06, 146–148 cm	14.47	351.6	45	63	49	19	34	1205	23	65	341	31	16	12	—	—
722B-2H-07, 06–08 cm	14.57	353.7	49	67	50	18	35	1183	25	71	360	21	13	13	—	—
722B-2H-07, 16–18 cm	14.67	356.0	45	61	51	17	33	1208	25	70	227	23	14	12	—	—
722B-2H-07, 26–28 cm	14.77	360.5	55	73	56	19	34	1115	29	73	237	23	13	14	—	—
722B-2H-07, 36–38 cm	14.87	365.0	46	72	53	20	36	1136	29	73	260	23	19	14	—	—

— Missing data or no data available.
[a] Chronostratigraphy from Clemens and Prell, pers. comm., March 1989.

APPENDIX C

Hole 724C Major Element Analyses. Corrected for Salt Contribution and Dilution.

Sample identification	Depth (mbsf)	[a]Age (k.y.)	Si (wt%)	Al (wt%)	Fe (wt%)	Mg (wt%)	Ca (wt%)	Na (wt%)	K (wt%)	Ti (wt%)	Mn (wt%)	P (wt%)
724C-1H-01, 25–27 cm	0.25	6.1	11.94	2.12	0.90	1.12	21.97	1.05	0.57	0.164	0.025	0.445
724C-1H-01, 45–47 cm	0.45	7.5	10.66	1.97	0.87	0.99	24.63	0.72	0.52	0.156	0.022	0.221
724C-1H-01, 65–67 cm	0.65	8.8	12.12	2.23	0.98	1.50	22.78	0.84	0.61	0.180	0.027	0.099
724C-1H-01, 85–87 cm	0.85	10.1	11.93	2.22	0.98	1.51	22.65	0.87	0.62	0.180	0.031	0.091
724C-1H-01, 105–107 cm	1.05	11.5	11.74	2.29	1.13	1.69	22.76	0.81	0.64	0.193	0.032	0.105
724C-1H-01, 125–127 cm	1.25	12.8	13.98	2.64	1.28	2.04	20.85	0.90	0.74	0.222	0.036	0.073
724C-1H-01, 145–147 cm	1.45	14.1	14.08	2.73	1.34	2.14	19.95	0.81	0.77	0.222	0.036	0.076
724C-1H-02, 15–17 cm	1.65	15.5	14.12	2.75	1.42	2.09	19.13	0.88	0.78	0.231	0.037	0.081
724C-1H-02, 35–37 cm	1.85	16.8	14.42	2.86	1.48	2.18	19.25	0.93	0.80	0.241	0.037	0.092
724C-1H-02, 55–57 cm	2.05	18.1	14.61	2.99	1.60	2.25	18.64	0.84	0.86	0.241	0.033	0.102
724C-1H-02, 75–77 cm	2.25	19.5	13.90	2.90	1.51	2.22	19.65	0.79	0.81	0.238	0.036	0.155
724C-1H-02, 95–97 cm	2.45	20.8	14.04	2.98	1.71	2.22	19.28	0.85	0.83	0.244	0.037	0.155
724C-2H-01, 10–12 cm	2.90	23.8	13.88	2.64	1.30	2.02	20.78	0.83	0.73	0.223	0.036	0.086
724C-2H-01, 25–27 cm	3.05	25.3	14.22	2.87	1.48	2.03	19.67	0.86	0.78	0.240	0.038	0.142
724C-2H-01, 45–47 cm	3.25	27.6	14.02	2.82	1.54	2.07	19.46	1.02	0.78	0.239	0.038	0.105
724C-2H-01, 65–67 cm	3.45	29.8	15.46	3.20	1.73	2.31	17.14	1.11	0.95	0.262	0.037	0.113
724C-2H-01, 85–87 cm	3.65	32.1	15.11	2.99	1.56	2.23	19.00	0.82	0.82	0.251	0.040	0.142
724C-2H-01, 105–107 cm	3.85	34.3	14.80	2.88	1.47	1.95	19.71	0.81	0.80	0.247	0.036	0.083
724C-2H-01, 125–127 cm	4.05	36.6	19.84	4.22	2.34	2.76	12.15	1.21	1.16	0.326	0.040	0.157
724C-2H-01, 145–147 cm	4.25	38.8	15.56	3.08	1.62	2.22	19.19	0.89	0.85	0.254	0.042	0.095
724C-2H-02, 15–17 cm	4.45	41.1	16.00	3.17	1.62	2.25	19.06	1.01	0.86	0.260	0.042	0.106
724C-2H-02, 35–37 cm	4.65	43.3	15.19	3.06	1.65	2.11	17.85	0.90	0.83	0.254	0.035	0.121
724C-2H-02, 55–57 cm	4.85	45.5	14.81	2.93	1.58	2.03	18.60	0.93	0.79	0.243	0.038	0.126
724C-2H-02, 75–77 cm	5.05	47.8	13.25	2.76	1.47	1.85	20.36	0.77	0.74	0.225	0.036	0.147
724C-2H-02, 95–97 cm	5.25	50.0	14.42	2.91	1.55	2.06	19.44	0.96	0.78	0.246	0.040	0.120
724C-2H-02, 115–117 cm	5.45	52.3	15.74	3.11	1.64	2.12	18.69	1.00	0.84	0.268	0.036	0.157
724C-2H-02, 135–137 cm	5.65	54.5	13.53	2.92	1.57	2.05	20.13	0.86	0.77	0.232	0.034	0.151
724C-2H-03, 05–07 cm	5.85	56.8	14.47	2.97	1.64	2.31	19.86	0.82	0.83	0.252	0.041	0.064
724C-2H-03, 25–27 cm	6.05	59.0	14.06	2.89	1.50	1.36	20.95	0.22	0.76	0.247	0.037	0.085
724C-2H-03, 45–47 cm	6.25	61.1	13.68	2.84	1.54	2.10	20.51	0.94	0.79	0.237	0.038	0.064
724C-2H-03, 65–67 cm	6.45	63.2	13.35	2.80	1.57	2.39	20.41	1.17	0.79	0.235	0.035	0.064
724C-2H-03, 85–87 cm	6.65	65.3	13.66	2.76	1.43	1.89	19.89	0.85	0.75	0.234	0.036	0.094
724C-2H-03, 105–107 cm	6.85	67.4	14.86	2.95	1.47	2.10	20.38	0.92	0.79	0.243	0.037	0.103
724C-2H-03, 125–127 cm	7.05	69.5	14.37	2.85	1.47	1.97	19.74	0.82	0.76	0.240	0.035	0.113
724C-2H-03, 145–147 cm	7.25	71.6	15.67	3.24	1.75	2.12	17.40	0.89	0.86	0.267	0.038	0.117
724C-2H-04, 15–17 cm	7.45	73.7	13.44	2.80	1.41	1.84	20.42	0.96	0.75	0.220	0.031	0.130
724C-2H-04, 35–37 cm	7.65	75.8	12.29	2.45	1.15	1.45	22.44	0.89	0.65	0.196	0.031	0.225
724C-2H-04, 55–57 cm	7.85	77.9	9.53	1.94	0.84	1.01	25.68	0.85	0.51	0.157	0.023	0.292
724C-2H-04, 75–77 cm	8.05	80.0	11.57	2.35	1.13	1.45	23.15	0.89	0.63	0.194	0.028	0.148
724C-2H-04, 95–97 cm	8.25	86.0	12.15	2.45	1.15	1.10	23.02	0.53	0.63	0.207	0.033	0.155
724C-2H-04, 115–117 cm	8.45	92.0	10.50	2.19	1.03	1.28	24.37	0.84	0.56	0.178	0.025	0.196
724C-2H-04, 135–137 cm	8.65	98.0	9.92	2.06	0.93	1.18	25.62	0.72	0.53	0.164	0.026	0.167
724C-2H-05, 05–07 cm	8.85	104.0	11.15	2.22	1.00	1.50	25.52	0.97	0.59	0.177	0.027	0.169
724C-2H-05, 25–27 cm	9.05	110.0	11.06	2.21	1.06	1.33	24.68	0.73	0.59	0.181	0.029	0.218
724C-2H-05, 45–47 cm	9.25	116.0	10.96	2.12	0.96	1.36	23.83	0.73	0.57	0.174	0.026	0.135
724C-2H-05, 65–67 cm	9.45	122.0	12.25	2.35	1.07	1.70	22.82	0.85	0.63	0.195	0.031	0.099
724C-2H-05, 85–85 cm	9.65	123.2	12.42	2.33	1.06	1.62	20.14	0.88	0.64	0.188	0.034	0.073
724C-2H-05, 105–107 cm	9.85	124.4	12.97	2.55	1.22	1.97	21.38	0.88	0.70	0.206	0.034	0.066
724C-2H-05, 125–127 cm	10.05	125.5	13.83	2.69	1.29	2.07	20.70	0.89	0.74	0.221	0.037	0.060
724C-2H-05, 145–147 cm	10.25	126.7	12.42	2.47	1.27	2.01	21.01	0.55	0.70	0.206	0.038	0.053
724C-2H-06, 15–17 cm	10.45	127.9	14.01	2.67	1.32	2.09	20.71	0.91	0.74	0.225	0.035	0.058
724C-2H-06, 35–37 cm	10.65	129.1	14.22	2.76	1.36	2.14	20.40	0.86	0.76	0.233	0.038	0.060
724C-2H-06, 55–57 cm	10.85	130.3	14.00	2.87	1.53	2.42	20.05	0.88	0.81	0.233	0.037	0.066
724C-2H-06, 75–77 cm	11.05	131.5	14.27	2.96	1.57	2.37	19.78	0.91	0.82	0.236	0.038	0.067
724C-2H-06, 95–97 cm	11.25	132.6	14.38	2.93	1.57	2.39	19.57	0.73	0.84	0.241	0.038	0.063
724C-2H-06, 115–117 cm	11.45	133.8	14.84	3.06	1.59	2.59	18.09	1.18	0.87	0.238	0.037	0.081
724C-2H-06, 135–137 cm	11.65	135.0	14.91	3.03	1.49	2.23	18.90	0.83	0.86	0.240	0.038	0.072
724C-2H-07, 05–07 cm	11.85	137.8	15.18	3.07	1.53	2.37	19.24	0.79	0.88	0.244	0.039	0.075
724C-2H-07, 25–27 cm	12.05	140.5	15.32	3.02	1.51	2.27	18.86	0.92	0.86	0.240	0.039	0.072
724C-2H-07, 45–47 cm	12.25	143.3	14.88	3.06	1.62	2.33	18.57	0.95	0.87	0.250	0.037	0.080
724C-2H-07, 60–62 cm	12.40	146.1	15.02	3.11	1.58	2.32	18.73	0.82	0.89	0.248	0.040	0.064
724C-3H-01, 25–27 cm	12.45	146.7	14.88	3.08	1.58	2.27	18.46	0.92	0.87	0.247	0.042	0.064
724C-3H-01, 45–47 cm	12.65	148.8	13.99	2.92	1.50	2.29	19.85	0.89	0.82	0.234	0.033	0.090
724C-3H-01, 65–67 cm	12.85	151.6	13.88	2.95	1.69	2.35	19.52	0.82	0.84	0.235	0.040	0.070
724C-3H-01, 85–87 cm	13.05	154.4	14.12	2.98	1.55	2.36	19.56	0.75	0.83	0.238	0.038	0.067
724C-3H-01, 105–107 cm	13.25	157.2	13.88	2.92	1.51	2.31	19.79	0.79	0.80	0.244	0.037	0.075
724C-3H-01, 125–127 cm	13.45	159.9	14.14	2.95	1.55	2.29	19.86	0.87	0.82	0.241	0.039	0.067
724C-3H-01, 145–147 cm	13.65	162.7	13.94	2.94	1.56	2.31	19.79	0.80	0.81	0.241	0.040	0.072
724C-3H-02, 15–17 cm	13.85	165.5	13.72	2.95	1.63	2.36	19.80	0.81	0.82	0.237	0.041	0.067
724C-3H-02, 35–37 cm	14.05	168.2	13.82	2.94	1.60	2.26	19.96	0.76	0.81	0.235	0.034	0.095
724C-3H-02, 55–57 cm	14.25	171.0	14.30	2.97	1.59	2.29	19.62	0.86	0.82	0.242	0.036	0.060
724C-3H-02, 75–77 cm	14.45	172.5	14.50	3.04	1.59	2.37	19.47	0.77	0.83	0.244	0.036	0.057
724C-3H-02, 95–97 cm	14.65	174.0	13.53	2.81	1.55	2.23	18.85	0.87	0.83	0.238	0.039	0.052
724C-3H-02, 115–117 cm	14.85	175.5	14.68	3.04	1.63	2.37	19.11	0.85	0.85	0.254	0.042	0.054
724C-3H-02, 135–137 cm	15.05	177.0	14.79	3.08	1.63	2.34	18.71	0.86	0.86	0.253	0.039	0.062
724C-3H-03, 05–07 cm	15.25	178.5	14.27	2.98	1.65	2.28	18.26	0.85	0.86	0.253	0.039	0.059
724C-3H-03, 25–27 cm	15.45	180.0	14.79	3.12	1.70	2.37	18.63	0.75	0.87	0.257	0.039	0.071

Appendic C (continued).

Sample identification	Depth (mbsf)	[a]Age (k.y.)	Si (wt%)	Al (wt%)	Fe (wt%)	Mg (wt%)	Ca (wt%)	Na (wt%)	K (wt%)	Ti (wt%)	Mn (wt%)	P (wt%)
724C-3H-03, 45–47 cm	15.65	181.5	15.80	3.44	1.91	2.22	18.32	0.56	0.94	0.269	0.044	0.076
724C-3H-03, 65–67 cm	15.85	183.0	14.91	3.32	1.84	2.50	17.46	0.77	0.93	0.263	0.038	0.077
724C-3H-03, 85–87 cm	16.05	185.1	14.88	3.25	1.86	2.54	17.99	0.82	0.91	0.263	0.041	0.075
724C-3H-03, 105–107 cm	16.25	187.2	16.79	3.65	2.00	2.69	15.16	0.98	1.02	0.291	0.042	0.087
724C-3H-03, 125–127 cm	16.45	189.3	19.34	4.17	2.34	3.25	21.68	1.27	1.17	0.321	0.051	0.084
724C-3H-03, 145–147 cm	16.65	191.5	15.17	3.32	1.90	2.53	17.87	0.88	0.93	0.265	0.042	0.071
724C-3H-04, 15–17 cm	16.85	193.6	15.50	3.33	1.86	2.48	17.80	0.96	0.94	0.270	0.041	0.063
724C-3H-04, 35–37 cm	17.05	195.7	15.48	3.38	1.92	2.49	17.84	0.84	0.93	0.272	0.044	0.059
724C-3H-04, 55–57 cm	17.25	197.8	17.21	3.88	2.14	2.79	14.69	1.01	1.08	0.308	0.046	0.077
724C-3H-04, 75–77 cm	17.45	199.9	15.31	3.38	1.88	2.45	17.36	0.74	0.95	0.265	0.042	0.059
724C-3H-04, 95–97 cm	17.65	202.0	15.34	3.32	1.83	2.44	18.10	0.90	0.92	0.267	0.045	0.067
724C-3H-04, 115–117 cm	17.85	204.2	15.26	3.40	1.91	2.55	17.49	0.92	0.94	0.269	0.044	0.068
724C-3H-04, 135–137 cm	18.05	206.3	16.19	3.60	2.02	2.50	16.09	0.93	0.97	0.278	0.039	0.097
724C-3H-05, 05–07 cm	18.25	208.4	15.87	3.42	1.97	2.38	16.89	1.03	0.93	0.280	0.041	0.089
724C-3H-05, 25–27 cm	18.45	210.5	14.09	3.10	1.75	2.28	19.37	1.00	0.84	0.251	0.040	0.292
724C-3H-05, 45–47 cm	18.65	212.6	14.11	3.13	1.73	2.14	19.25	0.82	0.85	0.251	0.038	0.097
724C-3H-05, 65–67 cm	18.85	214.7	14.53	3.12	1.71	2.21	19.06	0.86	0.85	0.248	0.040	0.102
724C-3H-05, 85–87 cm	19.05	216.8	13.20	2.90	1.68	2.14	19.12	0.78	0.83	0.259	0.038	0.074
724C-3H-05, 105–107 cm	19.25	219.0	13.54	3.01	1.70	2.09	19.71	0.89	0.82	0.245	0.041	0.092
724C-3H-05, 125–127 cm	19.45	221.1	14.15	3.04	1.64	2.14	19.04	0.92	0.81	0.247	0.034	0.126
724C-3H-05, 145–147 cm	19.65	223.2	14.62	3.11	1.68	2.22	18.98	0.83	0.85	0.256	0.038	0.129
724C-3H-06, 15–17 cm	19.85	225.3	14.21	3.10	1.70	2.21	18.95	0.97	0.83	0.248	0.034	0.166
724C-3H-06, 35–37 cm	20.05	227.4	9.10	2.02	1.01	1.21	25.46	0.70	0.53	0.162	0.025	0.289
724C-3H-06, 55–57 cm	20.25	229.5	9.90	2.17	1.15	1.32	24.00	0.72	0.58	0.176	0.024	0.494
724C-3H-06, 75–77 cm	20.45	231.7	11.25	2.46	1.29	1.54	22.66	0.83	0.66	0.197	0.027	0.269
724C-3H-06, 95–97 cm	20.65	233.8	6.85	1.57	0.79	0.97	28.27	0.63	0.41	0.128	0.020	0.547
724C-3H-06, 115–117 cm	20.85	235.9	10.41	2.39	1.30	1.66	23.38	0.69	0.66	0.191	0.028	0.134
724C-3H-06, 135–137 cm	21.05	238.0	11.29	2.58	1.43	1.77	22.57	0.72	0.71	0.204	0.031	0.080
724C-3H-07, 05–07 cm	21.25	239.2	12.42	2.72	1.45	1.82	21.70	0.70	0.75	0.220	0.035	0.084
724C-3H-07, 25–27 cm	21.45	240.3	12.73	2.67	1.40	1.83	21.30	0.84	0.74	0.227	0.035	0.089
724C-3H-07, 45–47 cm	21.65	241.5	12.88	2.71	1.42	1.75	21.14	0.77	0.73	0.218	0.031	0.153
724C-3H-07, 65–67 cm	21.83	242.5	12.02	2.53	1.28	1.63	21.83	0.83	0.68	0.207	0.028	0.207
724C-4H-01, 13–15 cm	21.85	242.6	12.41	2.40	1.15	1.58	22.37	0.78	0.65	0.204	0.028	0.104
724C-4H-01, 25–27 cm	21.95	243.2	12.04	2.38	1.20	1.54	22.64	0.73	0.65	0.201	0.029	0.125
724C-4H-01, 45–47 cm	22.15	244.4	12.80	2.51	1.26	1.66	21.23	0.78	0.72	0.219	0.031	0.091
724C-4H-01, 65–67 cm	22.35	245.5	14.79	2.97	1.50	2.09	19.17	0.90	0.83	0.249	0.034	0.079
724C-4H-01, 85–85 cm	22.55	246.7	15.21	3.16	1.68	2.26	18.19	0.85	0.89	0.260	0.038	0.080
724C-4H-01, 105–107 cm	22.75	247.8	15.60	3.27	1.73	2.36	16.83	0.96	0.93	0.265	0.032	0.087
724C-4H-01, 125–127 cm	22.95	249.0	14.10	3.03	1.68	2.09	18.92	0.88	0.85	0.242	0.032	0.090
724C-4H-01, 145–147 cm	23.15	254.4	16.10	3.22	1.69	2.34	17.13	1.00	0.90	0.281	0.035	0.094
724C-4H-02, 15–17 cm	23.35	259.9	14.89	3.03	1.64	2.17	18.42	0.90	0.85	0.255	0.035	0.093
724C-4H-02, 35–37 cm	23.55	265.3	14.67	3.05	1.72	2.18	18.25	0.88	0.84	0.251	0.032	0.127
724C-4H-02, 55–57 cm	23.75	270.7	14.64	3.09	1.63	2.21	19.09	0.77	0.87	0.251	0.039	0.102
724C-4H-02, 75–77 cm	23.95	276.1	14.12	3.03	1.61	2.18	19.38	0.82	0.85	0.245	0.033	0.091
724C-4H-02, 95–97 cm	24.15	281.6	14.57	3.14	1.81	2.27	19.14	0.78	0.88	0.251	0.038	0.095
724C-4H-02, 115–117 cm	24.35	287.0	14.51	3.13	1.72	2.27	18.98	0.93	0.88	0.254	0.036	0.092
724C-4H-02, 135–137 cm	24.55	289.2	12.73	2.78	1.54	2.10	21.27	0.76	0.79	0.226	0.033	0.057
724C-4H-03, 05–07 cm	24.75	291.4	13.01	2.85	1.54	2.15	21.05	0.76	0.82	0.230	0.035	0.066
724C-4H-03, 25–27 cm	24.95	293.6	12.80	2.72	1.45	1.90	21.23	0.82	0.75	0.221	0.031	0.077
724C-4H-03, 45–47 cm	25.15	295.8	12.63	2.68	1.39	1.97	21.52	0.77	0.77	0.220	0.034	0.065
724C-4H-03, 65–67 cm	25.35	298.0	12.24	2.66	1.42	1.99	21.71	0.75	0.77	0.216	0.033	0.058
724C-4H-03, 85–87 cm	25.55	300.2	12.00	2.57	1.38	1.83	21.36	0.77	0.75	0.212	0.031	0.062
724C-4H-03, 105–107 cm	25.75	302.4	13.13	2.79	1.45	1.79	22.46	0.83	0.75	0.227	0.031	0.095
724C-4H-03, 125–127 cm	25.95	304.6	12.30	2.61	1.30	1.61	20.70	0.76	0.71	0.211	0.031	0.099
724C-4H-03, 145–147 cm	26.15	306.8	13.96	2.86	1.39	1.80	21.37	0.82	0.77	0.230	0.031	0.128
724C-4H-04, 15–17 cm	26.35	309.0	12.18	2.53	1.23	1.53	22.64	0.84	0.68	0.204	0.025	0.138
724C-4H-04, 35–37 cm	26.55	311.2	10.72	2.18	1.02	1.26	24.25	0.65	0.59	0.176	0.024	0.139
724C-4H-04, 55–57 cm	26.75	313.4	10.90	2.26	1.06	1.42	26.59	0.79	0.60	0.175	0.025	0.173
724C-4H-04, 75–77 cm	26.95	315.6	11.05	2.22	1.00	1.32	24.18	0.76	0.61	0.184	0.024	0.127
724C-4H-04, 95–97 cm	27.15	317.8	11.95	2.29	0.98	1.30	23.32	0.70	0.63	0.190	0.025	0.142
724C-4H-04, 115–117 cm	27.35	320.0	11.96	2.36	1.10	1.45	23.10	0.74	0.65	0.197	0.025	0.194
724C-4H-04, 135–137 cm	27.55	322.2	10.73	2.20	1.04	1.36	23.93	0.80	0.60	0.178	0.025	0.271
724C-4H-05, 05–07 cm	27.75	324.4	10.50	2.12	0.99	1.25	18.89	0.76	0.57	0.171	0.023	0.533
724C-4H-05, 25–27 cm	27.95	326.6	8.26	1.33	0.86	1.19	26.42	0.63	0.47	0.141	0.022	0.272
724C-4H-05, 45–47 cm	28.15	328.8	11.63	2.18	1.08	1.58	23.32	0.73	0.65	0.192	0.026	0.140
724C-4H-05, 65–67 cm	28.35	331.0	12.65	2.42	1.14	1.72	22.19	0.80	0.66	0.200	0.032	0.100
724C-4H-05, 85–87 cm	28.55	332.7	11.54	2.29	1.07	1.67	23.44	0.74	0.63	0.191	0.030	0.099
724C-4H-05, 105–107 cm	28.75	334.3	12.04	2.46	1.23	1.92	23.00	0.68	0.67	0.207	0.031	0.066
724C-4H-05, 125–127 cm	28.95	336.0	11.44	2.32	1.11	1.76	24.66	0.75	0.63	0.189	0.026	0.102
724C-4H-05, 145–147 cm	29.15	337.7	12.71	2.51	1.26	1.98	21.94	0.65	0.70	0.208	0.032	0.048
724C-4H-06, 15–17 cm	29.35	339.3	12.74	2.56	1.27	2.02	21.74	0.76	0.73	0.214	0.033	0.054
724C-4H-06, 35–37 cm	29.55	341.0	13.84	2.69	1.37	2.04	20.77	0.81	0.79	0.226	0.033	0.054
724C-4H-06, 55–57 cm	29.75	342.7	13.88	2.72	1.34	2.07	20.67	0.88	0.78	0.224	0.034	0.054
724C-4H-06, 75–77 cm	29.95	344.3	14.18	2.73	1.32	2.06	20.09	0.80	0.79	0.232	0.035	0.056
724C-4H-06, 95–97 cm	30.15	346.0	15.02	2.93	1.43	2.18	19.60	0.93	0.84	0.239	0.036	0.065
724C-4H-06, 115–117 cm	30.35	349.3	14.30	2.88	1.45	2.02	19.48	0.91	0.82	0.239	0.036	0.069
724C-4H-06, 135–137 cm	30.55	352.3	14.24	2.83	1.42	1.99	20.00	0.87	0.80	0.238	0.034	0.077
724C-4H-07, 15–17 cm	30.85	355.6	13.76	2.78	1.52	1.96	20.31	0.80	0.80	0.239	0.031	0.086

Appendic C (continued).

Sample identification	Depth (mbsf)	[a]Age (k.y.)	Si (wt%)	Al (wt%)	Fe (wt%)	Mg (wt%)	Ca (wt%)	Na (wt%)	K (wt%)	Ti (wt%)	Mn (wt%)	P (wt%)
724C-4H-07, 35–37 cm	31.05	—	14.39	2.86	1.43	2.00	19.29	0.84	0.82	0.239	0.036	0.081
724C-4H-07, 55–57 cm	31.25	—	12.86	2.61	1.39	1.81	20.80	0.74	0.75	0.218	0.031	0.128
724C-4H-07, 75–77 cm	31.46	—	12.93	2.69	1.39	1.94	20.73	0.76	0.76	0.224	0.029	0.079
724C-5H-01, 10–12 cm	31.30	—	12.27	2.54	1.27	1.85	22.13	0.80	0.72	0.209	0.033	0.098
724C-5H-01, 25–27 cm	31.45	—	12.30	2.44	1.16	1.71	21.74	0.89	0.69	0.207	0.030	0.106
724C-5H-01, 45–47 cm	31.65	—	12.36	2.40	1.13	1.57	22.70	0.79	0.68	0.208	0.032	0.113
724C-5H-01, 65–67 cm	31.85	—	12.43	2.37	1.10	1.51	22.50	0.76	0.66	0.212	0.031	0.180
724C-5H-01, 85–87 cm	32.05	—	12.75	2.40	1.09	1.59	22.12	0.82	0.67	0.215	0.032	0.224
724C-5H-01, 105–107 cm	32.25	—	12.87	2.38	1.10	1.47	22.25	0.82	0.66	0.210	0.027	0.305
724C-5H-01, 125–127 cm	32.45	—	12.48	2.33	1.05	1.40	21.03	0.82	0.65	0.202	0.027	0.347
724C-5H-01, 145–147 cm	32.65	—	12.92	2.35	1.00	1.50	21.85	0.96	0.65	0.197	0.028	0.930
724C-5H-02, 15–17 cm	32.85	—	13.05	2.42	1.04	1.71	21.86	0.89	0.66	0.210	0.031	0.258
724C-5H-02, 35–37 cm	33.05	—	13.60	2.50	1.08	1.86	21.31	0.86	0.70	0.216	0.032	0.144
724C-5H-02, 55–57 cm	33.25	—	12.49	2.52	1.24	2.07	20.75	0.84	0.71	0.209	0.031	0.354
724C-5H-02, 75–77 cm	33.45	—	13.84	2.56	1.21	1.98	18.85	0.92	0.73	0.226	0.032	0.186
724C-5H-02, 95–97 cm	33.65	—	15.45	2.82	1.38	2.12	19.20	0.86	0.81	0.250	0.038	0.057
724C-5H-02, 115–117 cm	33.85	—	11.41	2.41	1.28	2.04	22.32	0.68	0.68	0.207	0.035	0.131
724C-5H-02, 135–137 cm	34.05	—	11.68	2.49	1.34	2.07	22.62	0.80	0.70	0.215	0.037	0.068
724C-5H-03, 05–07 cm	34.25	—	12.45	2.76	1.44	2.17	19.99	0.78	0.77	0.227	0.031	0.174
724C-5H-03, 25–27 cm	34.45	—	13.56	2.70	1.36	2.15	19.79	0.81	0.76	0.228	0.035	0.092
724C-5H-03, 45–47 cm	34.65	—	13.60	2.73	1.38	2.28	20.24	0.98	0.77	0.236	0.037	0.071
724C-5H-03, 65–67 cm	34.85	—	13.59	2.76	1.41	2.12	20.56	0.84	0.77	0.232	0.038	0.103
724C-5H-03, 85–87 cm	35.05	—	12.60	2.70	1.53	2.17	21.15	0.69	0.76	0.226	0.037	0.071
724C-5H-03, 105–107 cm	35.25	—	12.94	2.65	1.41	2.02	21.35	0.85	0.74	0.219	0.034	0.117
724C-5H-03, 125–127 cm	35.45	—	12.52	2.59	1.39	1.94	21.34	0.80	0.74	0.220	0.037	0.111
724C-5H-03, 145–147 cm	35.65	—	13.07	2.65	1.34	1.89	21.58	0.79	0.73	0.223	0.031	0.101
724C-5H-04, 15–17 cm	35.85	—	13.04	2.55	1.20	1.63	21.99	0.90	0.70	0.216	0.031	0.168
724C-5H-04, 35–37 cm	36.05	—	13.21	2.54	1.17	1.50	22.01	0.82	0.69	0.216	0.030	0.268
724C-5H-04, 55–57 cm	36.25	—	12.62	2.47	1.10	1.50	22.10	0.88	0.65	0.203	0.029	0.312
724C-5H-04, 75–77 cm	36.45	—	11.98	2.23	0.89	1.40	22.68	0.92	0.59	0.184	0.025	0.807
724C-5H-04, 95–97 cm	36.65	—	11.87	2.27	0.99	1.32	23.16	0.90	0.60	0.187	0.026	0.176
724C-5H-04, 115–117 cm	36.85	—	11.07	2.13	0.91	1.18	24.12	0.82	0.56	0.176	0.025	0.241
724C-5H-04, 135–137 cm	37.05	—	9.73	1.89	0.81	0.90	26.04	0.75	0.50	0.152	0.021	0.182
724C-5H-05, 05–07 cm	37.25	—	11.80	2.27	0.99	1.26	23.27	0.93	0.61	0.185	0.028	0.250
724C-5H-05, 25–27 cm	37.45	—	12.13	2.30	1.00	1.31	23.13	0.78	0.62	0.191	0.027	0.206
724C-5H-05, 45–47 cm	37.65	—	12.40	2.43	1.11	1.45	22.55	0.96	0.66	0.199	0.029	0.194
724C-5H-05, 65–67 cm	37.85	—	12.60	2.33	0.97	1.23	22.07	0.88	0.62	0.196	0.031	0.155
724C-5H-05, 85–87 cm	38.05	—	13.39	2.50	1.07	1.46	21.68	0.95	0.67	0.211	0.029	0.173
724C-5H-05, 105–107 cm	38.25	—	13.26	2.51	1.10	1.45	21.38	0.89	0.67	0.213	0.031	0.177
724C-5H-05, 125–127 cm	38.45	—	13.80	2.66	1.26	1.76	20.53	0.95	0.71	0.232	0.031	0.145
724C-5H-05, 145–147 cm	38.65	—	13.58	2.60	1.25	1.60	21.20	0.86	0.69	0.225	0.026	0.391
724C-5H-06, 15–17 cm	38.85	—	12.84	2.48	1.10	1.47	22.38	0.83	0.66	0.204	0.031	0.202
724C-5H-06, 35–37 cm	39.05	—	12.74	2.41	1.10	1.44	22.19	0.87	0.64	0.206	0.031	0.233
724C-5H-06, 55–57 cm	39.25	—	12.57	2.38	1.06	1.43	22.40	0.77	0.63	0.194	0.032	0.200
724C-5H-06, 75–77 cm	39.45	—	12.42	2.48	1.19	1.58	21.77	0.90	0.66	0.206	0.031	0.165
724C-5H-06, 95–97 cm	39.65	—	12.20	2.41	1.13	1.49	22.38	0.80	0.65	0.201	0.030	0.169
724C-5H-06, 115–117 cm	39.85	—	12.04	2.45	1.17	1.65	22.22	0.70	0.66	0.202	0.033	0.155
724C-5H-06, 135–137 cm	40.05	—	12.68	2.45	1.11	1.58	21.86	0.95	0.66	0.211	0.030	0.152
724C-5H-07, 05–07 cm	40.25	—	11.60	2.34	1.17	1.70	22.86	0.79	0.63	0.199	0.029	0.291
724C-5H-07, 25–27 cm	40.45	—	12.94	2.71	1.43	2.09	20.88	0.85	0.74	0.231	0.036	0.141
724C-5H-07, 45–47 cm	40.65	—	13.21	2.77	1.46	2.05	20.52	0.91	0.77	0.230	0.036	0.143
724C-5H-07, 60–62 cm	40.80	—	12.92	2.64	1.34	1.88	20.74	0.89	0.72	0.223	0.034	0.141
724C-6X-01, 05–07 cm	40.85	—	10.62	2.34	1.22	1.39	23.34	0.81	0.61	0.187	0.027	0.218
724C-6X-01, 25–27 cm	41.05	—	10.01	2.28	1.20	1.39	23.86	0.71	0.60	0.186	0.025	0.171
724C-6X-01, 45–47 cm	41.25	—	9.45	2.02	1.02	1.27	25.18	0.73	0.55	0.172	0.026	0.167
724C-6X-01, 65–67 cm	41.45	—	10.23	2.34	1.27	1.76	23.95	0.73	0.65	0.194	0.031	0.094
724C-6X-01, 85–87 cm	41.65	—	11.55	2.59	1.35	1.93	22.69	0.83	0.71	0.214	0.033	0.078
724C-6X-01, 105–107 cm	41.85	—	10.79	2.46	1.33	1.83	23.14	0.75	0.67	0.206	0.030	0.082
724C-6X-01, 125–127 cm	42.05	—	11.78	2.48	1.31	1.70	22.04	0.76	0.69	0.215	0.030	0.115
724C-6X-01, 145–147 cm	42.25	—	14.60	3.04	1.60	2.24	26.46	1.00	0.84	0.252	0.038	0.166
724C-6X-02, 15–17 cm	42.45	—	11.49	2.30	1.12	1.42	23.25	0.73	0.63	0.198	0.027	0.135
724C-6X-02, 35–37 cm	42.65	—	12.03	2.45	1.25	1.63	21.41	0.73	0.67	0.209	0.028	0.181
724C-6X-02, 55–57 cm	42.85	—	12.17	2.38	1.20	1.66	22.18	0.74	0.67	0.215	0.029	0.113
724C-6X-02, 75–77 cm	43.05	—	13.61	2.68	1.38	2.03	20.58	0.91	0.75	0.244	0.034	0.113
724C-6X-02, 95–97 cm	43.25	—	14.49	2.81	1.44	2.17	19.57	0.85	0.80	0.264	0.035	0.088
724C-6X-02, 115–117 cm	43.45	—	14.12	2.83	1.50	2.21	19.59	0.88	0.80	0.256	0.033	0.106
724C-6X-02, 135–137 cm	43.65	—	14.41	2.90	1.50	2.31	19.05	0.82	0.81	0.255	0.034	0.092
724C-6X-03, 05–07 cm	43.85	—	15.65	3.07	1.59	2.47	18.02	0.98	0.87	0.267	0.037	0.069
724C-6X-03, 25–27 cm	44.05	—	14.57	2.94	1.55	2.33	18.82	0.92	0.83	0.254	0.038	0.083
724C-6X-03, 45–47 cm	44.25	—	14.60	2.93	1.53	2.35	18.72	0.93	0.83	0.266	0.038	0.087
724C-6X-03, 65–67 cm	44.45	—	13.94	2.96	1.62	2.61	18.62	0.86	0.84	0.246	0.038	0.078
724C-6X-03, 85–87 cm	44.65	—	14.19	3.02	1.65	2.69	18.52	0.85	0.86	0.246	0.038	0.088
724C-6X-03, 105–107 cm	44.85	—	13.72	2.91	1.57	2.47	19.14	0.83	0.82	0.237	0.036	0.098
724C-6X-03, 125–127 cm	45.05	—	13.96	3.02	1.71	2.61	18.51	0.92	0.85	0.246	0.040	0.085
724C-6X-03, 145–147 cm	45.25	—	15.10	3.11	1.67	2.51	18.27	0.86	0.89	0.257	0.041	0.079
724C-6X-04, 15–17 cm	45.45	—	14.38	3.10	1.73	2.56	18.20	0.80	0.88	0.251	0.038	0.075
724C-6X-04, 35–37 cm	45.65	—	13.57	3.02	1.79	2.51	18.97	0.78	0.86	0.243	0.037	0.091
724C-6X-04, 55–57 cm	45.85	—	13.80	3.13	1.80	2.49	18.55	0.87	0.88	0.247	0.036	0.095

Appendic C (continued).

Sample identification	Depth (mbsf)	[a]Age (k.y.)	Si (wt%)	Al (wt%)	Fe (wt%)	Mg (wt%)	Ca (wt%)	Na (wt%)	K (wt%)	Ti (wt%)	Mn (wt%)	P (wt%)
724C-6X-04, 75–77 cm	46.05	—	13.04	2.93	1.74	2.30	19.07	0.77	0.83	0.237	0.037	0.104
724C-6X-04, 95–97 cm	46.25	—	13.60	2.98	1.69	2.36	19.03	0.77	0.84	0.243	0.037	0.095
724C-6X-04, 115–117 cm	46.45	—	13.77	3.06	1.75	2.40	19.36	0.85	0.87	0.248	0.035	0.092
724C-6X-04, 135–137 cm	46.65	—	13.29	2.95	1.69	2.46	19.66	0.87	0.84	0.241	0.036	0.091
724C-6X-05, 05–07 cm	46.85	—	13.90	3.09	1.76	2.59	18.63	1.04	0.88	0.244	0.036	0.083
724C-6X-05, 25–27 cm	47.05	—	13.53	3.15	1.80	2.40	19.03	0.66	0.89	0.255	0.039	0.077
724C-6X-05, 45–47 cm	47.25	—	14.03	3.12	1.77	2.46	18.81	0.84	0.89	0.257	0.039	0.073
724C-6X-05, 65–67 cm	47.45	—	15.49	3.34	1.76	2.50	18.54	0.97	0.92	0.260	0.040	0.066
724C-6X-05, 85–87 cm	47.65	—	14.62	3.24	1.82	2.51	18.83	0.80	0.91	0.263	0.038	0.074
724C-6X-05, 105–107 cm	47.85	—	14.96	3.27	1.84	2.49	18.24	0.89	0.92	0.270	0.043	0.067
724C-6X-05, 125–127 cm	48.05	—	15.27	3.30	1.83	2.38	17.97	0.95	0.92	0.270	0.045	0.070
724C-6X-05, 145–147 cm	48.25	—	14.95	3.24	1.86	2.44	17.89	0.89	0.90	0.273	0.044	0.068
724C-6X-06, 15–17 cm	48.45	—	14.39	3.19	1.77	2.27	18.28	0.79	0.88	0.261	0.039	0.076
724C-6X-06, 35–37 cm	48.65	—	14.85	3.36	2.03	2.43	18.16	0.86	0.94	0.267	0.042	0.072
724C-6X-06, 55–57 cm	48.85	—	15.87	3.63	2.04	2.54	15.40	1.01	1.00	0.292	0.036	0.101
724C-6X-06, 75–77 cm	49.05	—	15.61	3.38	1.87	2.14	17.87	0.69	0.94	0.268	0.044	0.067
724C-6X-06, 95–97 cm	49.25	—	11.66	2.54	1.33	1.90	21.72	0.79	0.70	0.211	0.029	0.114
724C-7X-01, 25–27 cm	50.75	—	15.67	3.33	1.94	2.37	17.76	0.93	0.94	0.274	0.043	0.069
724C-7X-01, 65–67 cm	51.15	—	11.22	2.48	1.30	2.08	22.04	0.67	0.70	0.205	0.029	0.157
724C-7X-01, 85–87 cm	51.35	—	12.57	2.76	1.43	2.25	20.95	0.77	0.78	0.223	0.029	0.162
724C-7X-01, 105–107 cm	51.55	—	11.97	2.79	1.54	2.55	19.74	0.69	0.81	0.221	0.035	0.081
724C-7X-01, 125–127 cm	51.75	—	11.93	2.61	1.45	2.25	20.09	0.73	0.75	0.215	0.031	0.109
724C-7X-02, 15–17 cm	52.15	—	13.11	2.91	1.61	2.60	19.96	0.75	0.84	0.239	0.043	0.062
724C-7X-02, 35–37 cm	52.35	—	13.29	2.91	1.61	2.61	19.98	0.74	0.84	0.242	0.039	0.063
724C-7X-02, 55–57 cm	52.55	—	13.00	2.84	1.52	2.36	20.12	0.89	0.81	0.235	0.038	0.084
724C-7X-02, 75–77 cm	52.75	—	13.75	3.03	1.66	2.63	19.39	0.76	0.88	0.246	0.038	0.058
724C-7X-02, 115–117 cm	53.15	—	13.55	2.94	1.58	2.44	19.79	0.85	0.84	0.241	0.034	0.071
724C-7X-02, 135–137 cm	53.35	—	13.99	3.06	1.65	2.58	19.24	0.70	0.89	0.243	0.041	0.060
724C-7X-03, 05–07 cm	53.55	—	14.08	3.03	1.65	2.58	18.99	0.82	0.89	0.252	0.036	0.061
724C-7X-03, 25–27 cm	53.75	—	14.28	3.05	1.66	2.61	19.00	0.95	0.90	0.256	0.041	0.055
724C-7X-03, 65–67 cm	54.15	—	13.95	3.02	1.57	2.27	19.57	0.58	0.85	0.245	0.039	0.077
724C-7X-03, 85–87 cm	54.35	—	14.22	3.03	1.62	2.45	19.37	0.80	0.88	0.249	0.039	0.062
724C-7X-03, 105–107 cm	54.55	—	13.62	2.94	1.55	2.61	19.26	1.08	0.85	0.243	0.035	0.063
724C-7X-03, 125–127 cm	54.75	—	12.74	2.82	1.52	2.63	19.85	0.98	0.82	0.240	0.034	0.071
724C-7X-04, 15–17 cm	55.15	—	12.49	2.64	1.44	2.15	20.84	0.75	0.75	0.224	0.030	0.188
724C-7X-04, 35–37 cm	55.35	—	12.60	2.60	1.30	1.86	20.87	0.80	0.72	0.220	0.032	0.159
724C-7X-04, 55–57 cm	55.55	—	11.92	2.49	1.25	1.74	21.75	0.87	0.69	0.208	0.027	0.115
724C-7X-04, 75–77 cm	55.75	—	11.21	2.36	1.25	1.54	22.82	0.84	0.64	0.196	0.025	0.113
724C-7X-04, 115–117 cm	56.15	—	10.99	2.27	1.12	1.55	23.13	0.71	0.63	0.188	0.029	0.117
724C-7X-04, 135–137 cm	56.35	—	10.89	2.29	1.16	1.57	23.29	0.74	0.63	0.193	0.028	0.124
724C-7X-05, 05–07 cm	56.55	—	11.27	2.56	1.39	1.94	22.05	0.76	0.72	0.202	0.030	0.130
724C-7X-05, 25–27 cm	56.75	—	11.71	2.54	1.40	1.89	21.56	0.77	0.71	0.205	0.030	0.105
724C-7X-05, 65–67 cm	57.15	—	10.95	2.26	1.13	1.54	22.35	0.68	0.63	0.191	0.029	0.111
724C-7X-05, 85–87 cm	57.35	—	13.48	2.86	1.53	2.16	20.31	0.86	0.82	0.235	0.034	0.077
724C-7X-05, 105–107 cm	57.55	—	12.31	2.62	1.35	1.93	20.98	0.78	0.73	0.215	0.031	0.103
724C-7X-05, 125–127 cm	57.75	—	12.52	2.59	1.28	1.78	21.50	0.86	0.72	0.215	0.030	0.097
724C-7X-06, 15–17 cm	58.15	—	11.78	2.23	1.06	1.24	23.66	0.80	0.61	0.194	0.030	0.089
724C-7X-06, 35–37 cm	58.35	—	11.79	2.25	1.06	1.24	22.81	0.85	0.62	0.195	0.028	0.112
724C-7X-06, 55–57 cm	58.55	—	10.95	2.35	1.20	1.36	23.02	0.81	0.63	0.194	0.029	0.115
724C-7X-06, 75–77 cm	58.75	—	11.86	2.34	1.09	1.40	23.79	0.85	0.63	0.189	0.029	0.118
724C-8X-01, 05–07 cm	60.25	—	9.45	2.10	1.06	1.16	24.85	0.68	0.56	0.172	0.028	0.132
724C-8X-01, 25–27 cm	60.45	—	11.59	2.39	1.14	1.43	23.16	0.62	0.66	0.196	0.030	0.113
724C-8X-01, 65–67 cm	60.85	—	10.42	2.30	1.18	1.41	23.50	0.75	0.62	0.188	0.025	0.124
724C-8X-01, 85–87 cm	61.05	—	10.45	2.31	1.18	1.36	23.82	0.79	0.62	0.191	0.027	0.124
724C-8X-01, 105–107 cm	61.25	—	11.14	2.37	1.16	1.41	23.24	0.74	0.64	0.194	0.028	0.102
724C-8X-01, 125–127 cm	61.45	—	11.08	2.39	1.23	1.62	22.86	0.94	0.65	0.196	0.029	0.148
724C-8X-02, 15–17 cm	61.85	—	10.95	2.22	1.04	1.20	23.67	0.72	0.59	0.185	0.027	0.110
724C-8X-02, 35–37 cm	62.05	—	11.70	2.54	1.31	1.60	22.18	0.78	0.69	0.205	0.031	0.108
724C-8X-02, 55–57 cm	62.25	—	11.66	2.42	1.20	1.66	22.30	0.83	0.65	0.198	0.028	0.106
724C-8X-02, 75–77 cm	62.45	—	10.81	2.32	1.21	1.51	22.58	0.74	0.63	0.192	0.030	0.134
724C-8X-02, 115–117 cm	62.85	—	11.73	2.69	1.53	2.09	20.87	0.78	0.75	0.217	0.032	0.130
724C-8X-02, 135–137 cm	63.05	—	13.61	3.08	1.85	2.56	19.19	0.87	0.87	0.245	0.040	0.086
724C-8X-03, 05–07 cm	63.25	—	14.59	3.26	1.89	2.62	18.44	0.84	0.92	0.260	0.042	0.059
724C-8X-03, 25–27 cm	63.45	—	14.57	3.24	1.90	2.57	18.18	0.77	0.92	0.264	0.045	0.055
724C-8X-03, 65–67 cm	63.85	—	14.73	3.27	1.86	2.45	18.13	0.85	0.92	0.268	0.040	0.064
724C-8X-03, 85–87 cm	64.05	—	14.90	3.19	1.81	2.41	18.45	0.84	0.87	0.269	0.043	0.062
724C-8X-03, 105–107 cm	64.25	—	14.66	3.20	1.77	2.29	18.22	0.85	0.88	0.257	0.042	0.079
724C-8X-03, 125–127 cm	64.45	—	14.75	3.17	1.80	2.35	18.38	0.90	0.86	0.270	0.040	0.082
724C-8X-04, 15–17 cm	64.85	—	13.47	3.15	1.87	2.33	19.22	0.84	0.87	0.247	0.035	0.089
724C-8X-04, 35–37 cm	65.05	—	14.14	3.24	1.84	2.27	18.78	0.91	0.87	0.257	0.040	0.090
724C-8X-04, 75–77 cm	65.45	—	13.62	3.20	1.85	2.11	18.95	0.82	0.86	0.252	0.038	0.111
724C-8X-04, 95–97 cm	65.65	—	11.90	2.88	1.68	1.83	21.18	0.82	0.77	0.221	0.031	0.122
724C-8X-04, 115–117 cm	65.78	—	11.77	2.84	1.56	1.70	21.66	0.77	0.74	0.215	0.028	0.136
724C-8X-04, 135–137 cm	66.05	—	10.72	2.61	1.52	1.68	20.46	0.83	0.69	0.205	0.028	0.159
724C-8X-05, 05–07 cm	66.25	—	13.37	3.21	1.83	1.91	17.28	0.91	0.84	0.243	0.032	0.227
724C-8X-05, 25–27 cm	66.45	—	12.23	2.99	1.76	1.87	19.84	0.86	0.77	0.229	0.032	0.162
724C-8X-05, 65–67 cm	66.85	—	12.27	2.81	1.68	2.14	20.52	0.57	0.78	0.228	0.033	0.079
724C-8X-05, 85–87 cm	67.05	—	9.09	2.13	1.23	1.74	25.20	0.75	0.58	0.175	0.027	0.098

Appendic C (continued).

Sample identification	Depth (mbsf)	[a]Age (k.y.)	Si (wt%)	Al (wt%)	Fe (wt%)	Mg (wt%)	Ca (wt%)	Na (wt%)	K (wt%)	Ti (wt%)	Mn (wt%)	P (wt%)
724C-8X-05, 105-107 cm	67.25	—	12.68	2.93	1.76	2.38	19.7 9	0.78	0.81	0.234	0.038	0.068
724C-8X-05, 125-127 cm	67.45	—	12.99	2.99	1.75	2.34	19.92	0.73	0.82	0.246	0.036	0.072
724C-8X-06, 15-17 cm	67.85	—	15.75	3.35	1.85	2.36	16.99	1.01	0.89	0.275	0.041	0.106
724C-8X-06, 35-37 cm	68.05	—	12.46	2.99	1.74	2.12	19.80	0.96	0.82	0.232	0.031	0.100
724C-8X-06, 49-51 cm	68.19	—	10.75	2.52	1.48	1.78	22.05	0.63	0.69	0.201	0.028	0.092

— No data available.
[a] Chronostratigraphy from Zahn and Pedersen (this volume).

APPENDIX D
Elemental Statistics: Minimum, Average, and Maximum Values.

Hole 722B major elements.

	Si (wt%)	Al (wt%)	Fe (wt%)	Ca (wt%)	Ti (wt%)	Mn (wt%)	P (wt%)
Min.	4.48	1.11	0.70	21.40	0.07	0.02	0.03
Avg.	8.33	2.11	1.32	27.48	0.15	0.03	0.05
Max.	12.61	3.28	3.13	32.94	0.23	0.04	0.07

Hole 722B trace elements.

	Ni (ppm)	Cr (ppm)	V (ppm)	Cu (ppm)	Zn (ppm)	Sr (ppm)	Rb (ppm)	Zr (ppm)	Ba (ppm)	Ce (ppm)	Nd (ppm)	Y (ppm)	U (ppm)	Th (ppm)
Min.	31	30	31	15	25	740	12	33	118	6	7	10	2	1
Avg.	54	79	53	23	41	1064	26	62	380	23	16	14	3	2
Max.	83	143	81	41	62	1489	41	94	1046	41	23	19	5	4

Hole 724C major elements.

	Si (wt%)	Al (wt%)	Fe (wt%)	Mg (wt%)	Ca (wt%)	Na (wt%)	K (wt%)	Ti (wt%)	Mn (wt%)	P (wt%)
Min.	6.85	1.33	0.79	0.90	12.15	0.22	0.41	0.13	0.02	0.05
Avg.	13.20	2.75	1.44	1.98	20.65	0.83	0.76	0.23	0.03	0.12
Max.	19.84	4.22	2.34	3.25	28.27	1.27	1.17	0.33	0.05	0.93